

**The Federal Service for Hydrometeorology  
and Environmental Monitoring (ROSHYDROMET)**

**The Federal State Institution “The Russian Federation Hydrometeorological Research Center**

**The Federal State Budgetary Institution “Central Aerological Observatory”**

**Methodology Recommendations  
for the use of data from MTP-5 profiler**

**Moscow, 2010**

The methodology recommendations for the use of measurements of MTP-5 profilers have been prepared by the Federal State Institution “The Russian Federation Hydrometeorological Center”<sup>1</sup> in cooperation with the Federal State institution “The Central Aerological Observatory”<sup>2</sup>.

Principal Investigators:

I.N. Kuznetsova, PhD <sup>1</sup>

M.I. Nakhayev, PhD <sup>1</sup>

E.N. Kadygrov, Dr. of Sc., PhD <sup>2</sup>

E.A. Miller, Senior Scientist, PhD <sup>2</sup>

	<b>Contents</b>	<b>Page</b>
	<b>Introduction</b>	
1.	Establishing thermal state characteristics in a measurement layer	
<b>1.1.</b>	<b>Thermal stratification type</b>	
<b>1.2</b>	<b>Vertical temperature gradient</b>	
<b>1.3</b>	<b>Mixing layer height</b>	
<b>1.4</b>	<b>Inversion parameters</b>	
<b>2</b>	<b>Thermal state characteristics in a given interval</b>	
<b>2.1</b>	<b>Thermal stability type</b>	
<b>2.2</b>	<b>Temperature inversion duration, boundaries and magnitude</b>	
<b>2.3</b>	<b>Mixing layer mean and characteristic heights</b>	
<b>3</b>	<b>Analysis of diurnal temperature variation anomalies</b>	
<b>3.1</b>	<b>Passage of cold atmospheric front</b>	
<b>3.2</b>	<b>Secondary cold front</b>	
<b>3.3</b>	<b>Warm atmospheric front</b>	
<b>3.4</b>	<b>Diurnal temperature invariability</b>	
<b>3.5</b>	<b>Air mass advection</b>	
<b>3.6</b>	<b>Variable cloud amount and air-mass precipitation</b>	
<b>4.</b>	<b>Temperature inversion</b>	
<b>4.1</b>	<b>Radiation (surface) inversion</b>	
<b>4.2</b>	<b>Elevated temperature inversion. Urban inversion</b>	
<b>4.3</b>	<b>Advection temperature inversion</b>	
<b>4.4</b>	<b>Subsidence inversion</b>	
<b>4.5</b>	<b>Evaporation inversion</b>	
<b>4.6</b>	<b>Aerosol heating inversion</b>	
<b>5.</b>	<b>Identification of icing thermal conditions</b>	
<b>6.</b>	<b>The use of MTP-5 data in analyzing and forecasting meteorological pollution accumulation conditions</b>	
	<b>Conclusion</b>	
	<b>Supplement 1</b>	

## INTRODUCTION

The lower atmospheric layer as opposed to the rest of the atmosphere is characterized by significant intra-diurnal variability of all meteorological characteristics. Monitoring its state using conventional technology, i.e. radio sounding, is incompatible with the space and time scale of this variability.

Measuring system MTP-5 (microwave temperature profiler) enables mapping the thermal structure of the lower 600-m atmospheric layer and obtaining its time dynamics. This Handbook provides methodology of how to acquire skills in diagnosing atmospheric processes using visualized MTP-5 measurements

### **This methodological handbook is meant for:**

- operational use by synoptic meteorologists;
- forecasting weather conditions and air pollution;
- researching into atmospheric processes in the boundary layer.

### **The methodological recommendations given herein describe general approaches to analyzing visualized MTP-5 measurements, aiming at:**

- **analyzing atmospheric processes based on synoptic information:** specifying and detailing atmospheric processes, recognizing signs of weather changes and preconditions for disastrous phenomena;

- **evaluation and prediction of weather conditions favoring atmospheric pollution:** establishing the rate of variability of atmospheric processes as well as diagnosing and assessing the usefulness and feasibility of the inertial forecast of thermal stability;

- **investigation of the peculiarities of processes in the atmospheric boundary layer:** acquiring quantitative thermal characteristics, identifying lower atmosphere phenomena and processes in the MTP-5 visualized measurement data.

### **The Recommendations provide for analyzing MTP-5 data of 2 types:**

- a) stationary / mobile observations without using archived data;
- b) MTP-5 measurement data accumulated for a period of not less than a year aimed at making conclusions about thermal state variability for various weather types in separate seasons.

**The guidebook comprises recommendations for:**

- establishing thermal characteristics at a given time (Part 1);
- obtaining average characteristics for a certain single period (Part 2);
- identifying atmospheric processes of different scales and various atmospheric phenomena (Part 3);
- analyzing temperature inversions (Part 4);
- successive analysis of the lower atmosphere processes in assessing weather conditions associated with air pollution (Part 6); and

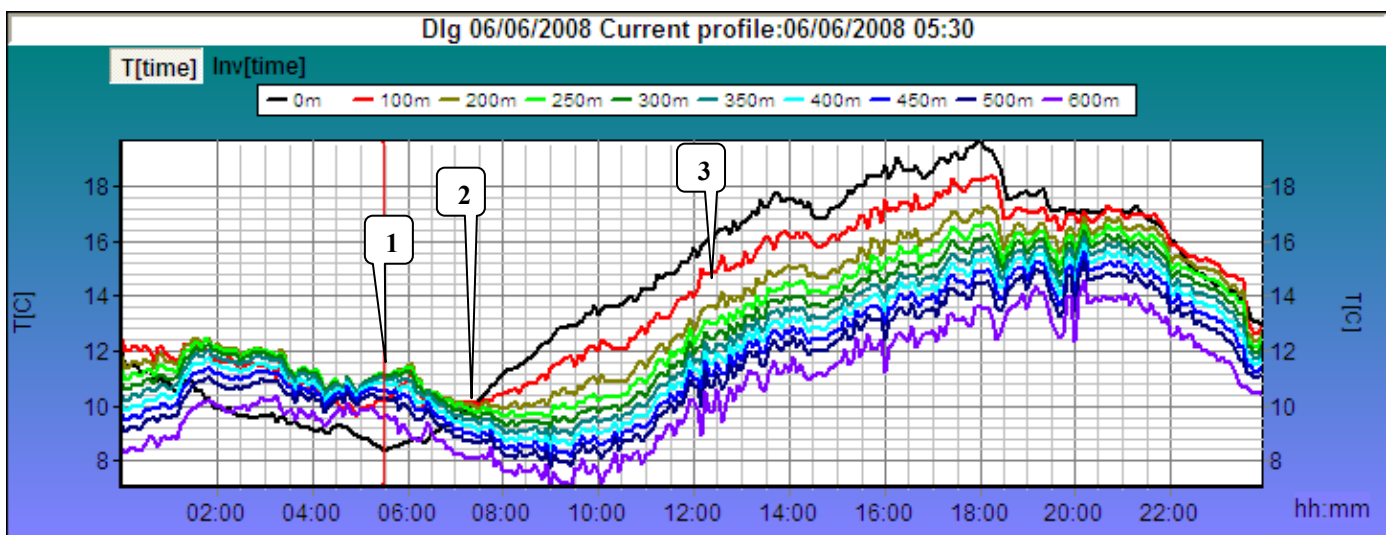
**Supplement 1. Correspondence between stability grades and thermal stratification**

The basic methodological approach of this handbook is based on brief descriptions of atmospheric processes illustrated by visualized MTP-5 data. Some of the illustrations are supplied with descriptions of separate events that enable detailed analysis of process dynamics and teach how to identify such phenomena or determine their characteristics. Many of the atmospheric processes are treated in terms of air mass change as a factor of anthropogenic species removal from surface air.

**1. Establishing thermal state characteristics in a measurement layer**

**1.1. Thermal stratification type**

To make analysis, the window “Profile” is used in which a dry adiabat profile is displayed and stratification type – unstable, neutral or stable – is defined (Fig.1). Thermal stratification type is evaluated at times indicated in a “thermogram” window as an elapsed-time meter pointer moves across the window “Profile”, using a dry adiabat reconstructed from surface temperature.



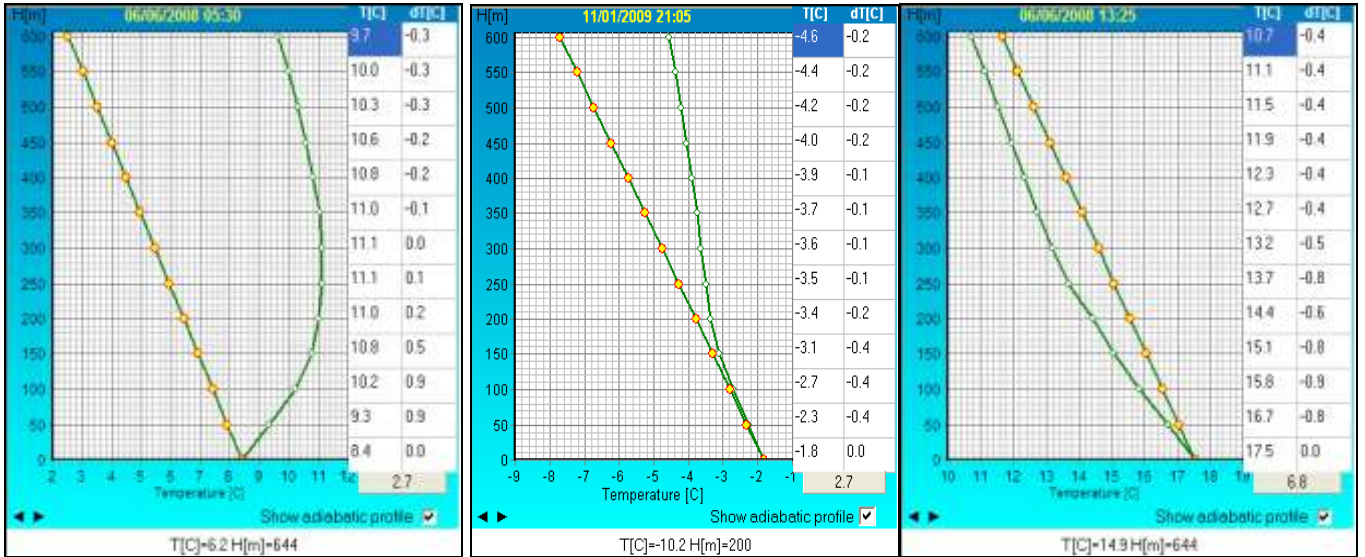


Fig.1 Diurnal temperature variability (top) in a 0-600 m layer in the form of thermograms and 3 stratification types: 1- stable (bottom left ), 2- neutral (center), and 3- unstable (right). In the figures below, the straight lines with circle markers indicate dry adiabats.

### 1.2 Vertical temperature gradient

In the window “Profile” (right), temperatures at levels from the surface up to 600 (1000) meters are presented with a 50-m interval (Fig.1 below). Generally, to characterize thermal state, temperature gradient is determined either in the surface layer (1-100 m) by formula (1) or in a layer of given thickness ( $h_i - h_{i+n}$ ) as temperature difference for  $h_i$  and  $h_{i+n}$  levels, which is normalized to the thickness of the layer concerned,  $(i)-(i+n)$ , in hundreds of meters, by formula (2).

$$\gamma_{(0-100)} (\text{°C}/100 \text{ M})= T(0) -T(100) \tag{1}$$

$$\gamma_{(h_i - h_{i+n})} (\text{°C}/100 \text{ M})= T(h_i) -T(h_{i+n}) /0.01(h_i - h_{i+n}) \tag{2}$$

### 1.3 Mixing layer height

In a general form, a mixing layer is conditioned by the height of the lower boundary of potential temperature inversion elevated to above a convective layer.

Graphically, determination of the height (thickness) of a mixing layer (MLH) consists in establishing the level of thermal stratification intersection with a dry adiabat reconstructed from surface temperature (in the case of relative humidity exceeding 92%, with a wet adiabat). Allowing for an MTP-5 temperature measurement error, in determining MLH, an additional layer starting from the intersection of a thermal stratification curve with a dry adiabat appears in the window “Temperature profile”, temperature difference between the lines becoming less than  $0.5\text{°C}$ .

Figure 2 represents all basic stratification types. In the case of surface inversion, MLH is not presented (Fig.2a), while with an elevated inversion MLH is determined starting from the point of stratification intersection with a dry adiabat onward, including a layer with stratification departure from a dry adiabat by not more than 0.5°C (Fig.2b). In the case of a low thermal stability (Fig.2c), as is also in the case of isothermalcy (Fig. 2f), MLH is the height of the layer with stratification departure from a dry adiabat by not more than 0.5°C. If thermal stratification throughout MTP-5 measurement layer localizes on a dry adiabat left, MLH exceeds the thickness of the measurement layer and is estimated to be more than 600 m.

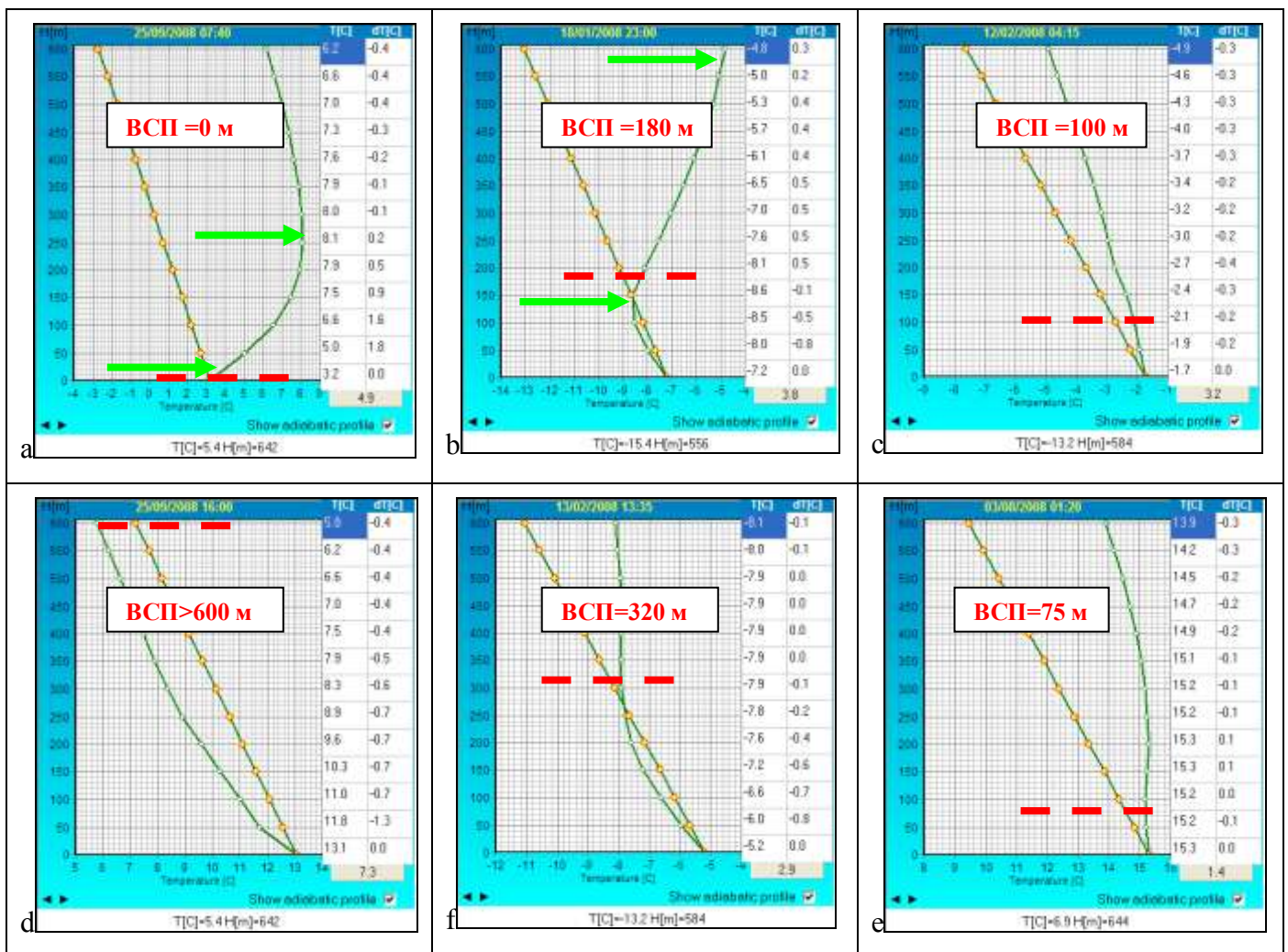


Figure 2 – MLH for different types of thermal stratification (red dashed line). Green arrows show temperature inversion boundaries.

To use MLH as a predictor one can employ Zilitinkevich formula

$$MLH = \chi(u_* L f^{-1})^{0.5} \quad (3)$$

where  $\chi = 0.4$  - is Karman constant;

$u_*$  = friction rate (dynamic rate);  
 $L$  is Monin-Obukhov length scale characterizing surface layer stratification;  
 $f=2\omega \sin\varphi$  is Coriolis parameter .

For a neutrally stratified stationary atmospheric surface layer

$$\mathbf{MLH} = \alpha \mathbf{0.4(u_* L f^1)^{0.5}} \quad (4)$$

where  $\alpha$  is an empirical coefficient which, depending on stratification type, varies between 0.05 and 0.4. In summer, under moderate or strong instability  $\alpha = 0.8$ .

To roughly estimate MLH one can use formula

$$\mathbf{MLH} = \alpha \mathbf{u_* f^{-1}} \quad (5)$$

In middle latitudes  $f = 10^{-4} \text{ s}^{-1}$

For winter conditions with neutral or weakly stable stratification (at  $\alpha=0.185$  and  $z_0=0.05$  m)

$$\mathbf{MLH} \approx \mathbf{125 U_{10}} \quad (6)$$

where  $U_{10}$  is the mean wind speed at a 10-m level.

### 1.4 Inversion parameters

In the case of an inversion temperature profile (temperature increase with height), in the window “Profile” inversion characteristics are defined: the lower and upper boundaries ( $LB_{inv}$ ,  $UB_{inv}$ , m) and the quantity ( $\Delta T_{inv}$ , °C).

**Note.** With MTP-5 temperature measurement error of about 0.5°C, inversion layer boundaries are determined from the level of non-fulfillment of temperature increase/decrease conditions.

In order to characterize the inversion, a stable stratification observed for not less than an hour is selected and its parameters are determined. In Fig. 2, the green arrows show inversion boundaries. In Fog.2a where surface inversion is presented,  $LB_{inv} = 0$  m,  $UB_{inv} = 250$  m, and  $\Delta T_{inv} = 4.9^\circ\text{C}$ . An elevated inversion displayed in Fig.2b has the following characteristics:  $LB_{inv} = 150$  m,  $UB_{inv} > 600$  m, and  $\Delta T_{inv} = 3.9^\circ\text{C}$ .

## 2. Thermal state characteristics in a given measurement interval

### 2.1 Thermal stability type

In the lower atmospheric layer, the most pronounced variations take place throughout the day. The characteristics of atmospheric boundary layer processes that determine the transport of substances from the earth surface often need to be established. It is recommended to assess the type of stratification in typical periods of the day - night, morning, daytime, and evening:

- cold season: night (07.00 p.m. – 07.00 a.m.), morning (07.00 a.m. – 10.00 a.m.), daytime (11.00 a.m. - 04.00 p.m.) and evening (04.00 p.m. – 07.00p.m.) (local time);
- warm season: night (10.00 p.m. – 06.00 a.m.), morning (06.00 a.m. – 09.00 a.m.), daytime (10.00 a.m.- 07.00p.m.), and evening (07.00 p.m. – 10.00 p.m.).

For each of the period, the type of which prevails in terms of duration or that prevailing in the second half of the period concerned is established:

- *stable* (inversion) with surface layer temperature gradient

$$\gamma_{100} < 0^{\circ}\text{C}/100\text{ m} \quad (7)$$

- *weakly stable* with surface layer temperature gradient

$$0^{\circ}\text{C}/100\text{ m} \leq \gamma_{100} < 0.98^{\circ}\text{C}/100\text{ m} \quad (8)$$

- *unstable* with surface layer temperature gradient

$$\gamma_{100} \geq 0.98^{\circ}\text{C}/100\text{ m} \quad (9)$$

**Note.** At relative air humidity over 92%, type is:

- *weakly stable* with surface layer temperature gradient  $0^{\circ}\text{C}/100\text{ m} \leq \gamma_{100} < 0.6^{\circ}\text{C}/100\text{ m}$  (10)

- *unstable* surface layer temperature gradient  $\gamma_{100} \geq 0.6^{\circ}\text{C}/100\text{ m}$  (11)

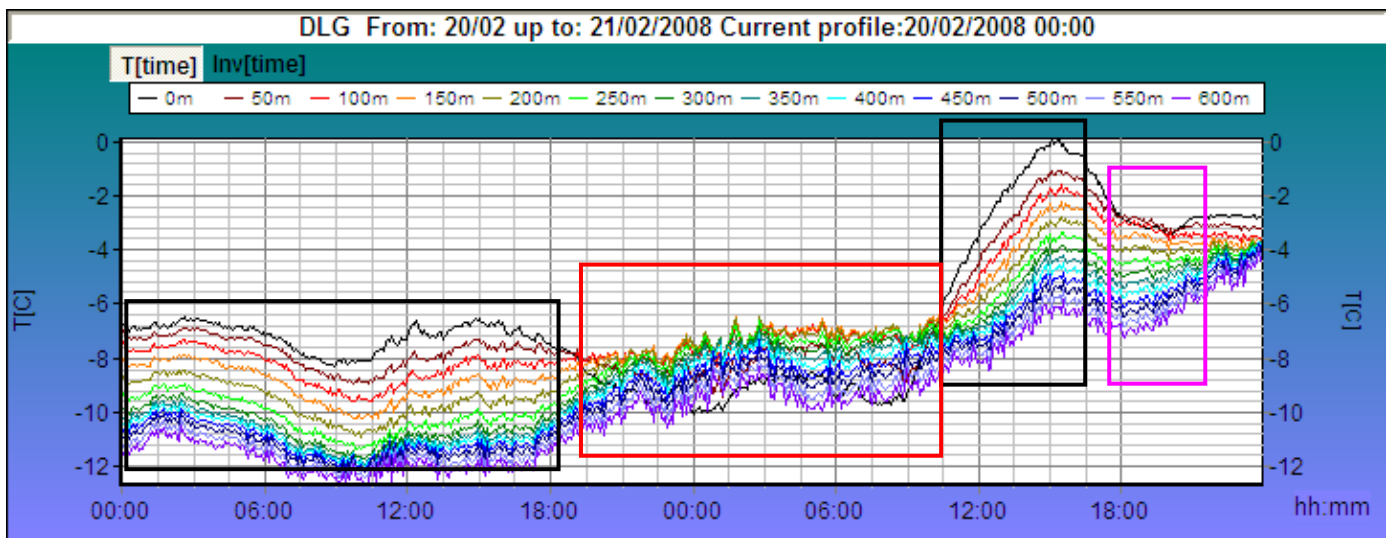


Fig.3. In the diurnal variation of thermal stratification (2 days) periods of thermal instability are outlined in black, stability in red, and weak stability in pink.

## 2.2 Temperature inversion duration, boundaries and magnitude

To determine the duration of temperature inversion, the dates of the beginning of its formation and its destruction are spliced: in a warm season, generally, two days (the previous and the current ones); in winter, inversions can persist for 5-6 days and in rare cases for up to 8 or more days.

In problems connected with the investigation of inversions, the duration is determined from the moment of inversion formation till its destruction. To explore inversion relations with impurities measured in discrete time periods, the duration is determined for established intervals preceding the time

of the concentration measurements. It is common knowledge that temperature inversions are subdivided into radiation-, advection-, subsidence-, and mixed types.

**Radiation (surface) inversions** are formed at sunset and destroyed at sunrise. Most often surface inversion is formed within less than an one hour and destroyed within 1-2 hours. With this in mind, **surface inversion duration** (in hours) is estimated for an interval between inversion temperature profile occurrence and the appearance of adiabatic temperature gradient in the lower 100-m layer, which marks the transition to convective mixing in the lower layer (Fig.4). The lower boundary of surface inversion is taken as 0 m with the upper boundary determined either by the inversion magnitude prevailing (modal) throughout the period of its existence or in the period of its maximal development; depending on the approach, the magnitude of inversion is determined: this is either the mean value for the period of prevailing inversion magnitude or the largest one for the period of maximum inversion development.

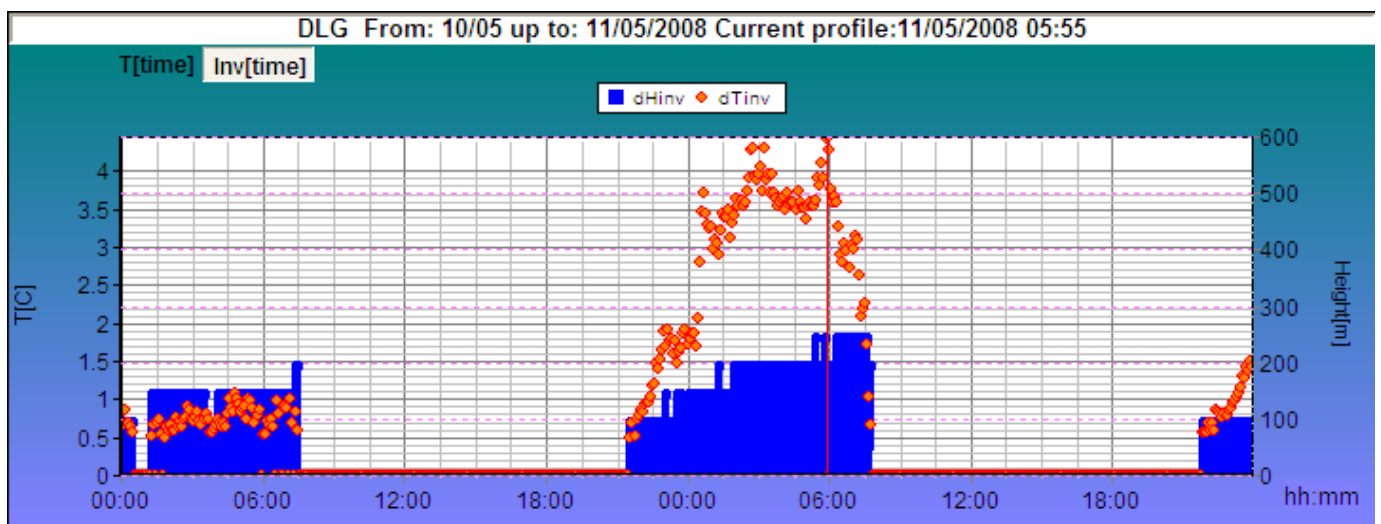


Fig.4. Temperature inversion characteristics. *The duration of the 10 May nighttime inversion was 7.5 hours with the lower boundary at 0 m, the upper boundary at 150 m, and a magnitude of 0.8°C (maximum 1°C). The 11 May inversion formed in the evening of the day before (21:00) and persisted till 07:00, hence a 10-hour duration. The characteristic magnitude of inversion on 11 May was 3.5°C (maximum 4.5°C) with the characteristic upper boundary at 200 m (175 m on average).*

**Advection inversions** are due to warm air overrunning colder air, including the frontal inversion of a warm front. The duration and characteristics of an elevated inversion are determined as follows:

- the duration is estimated (in hours) ;
- with the lower boundary changing within the range of 100-150 m, it is determined by the prevailing height for a set time interval (Fig. 22; Jan. 9).
- with the lower boundary varying within a wide height range, the mean value for the period concerned is determined.

In Fig. 5 are presented episodes of advection temperature inversion which is basically characterized by temperature rise at the highest MTP-5 measurement levels.

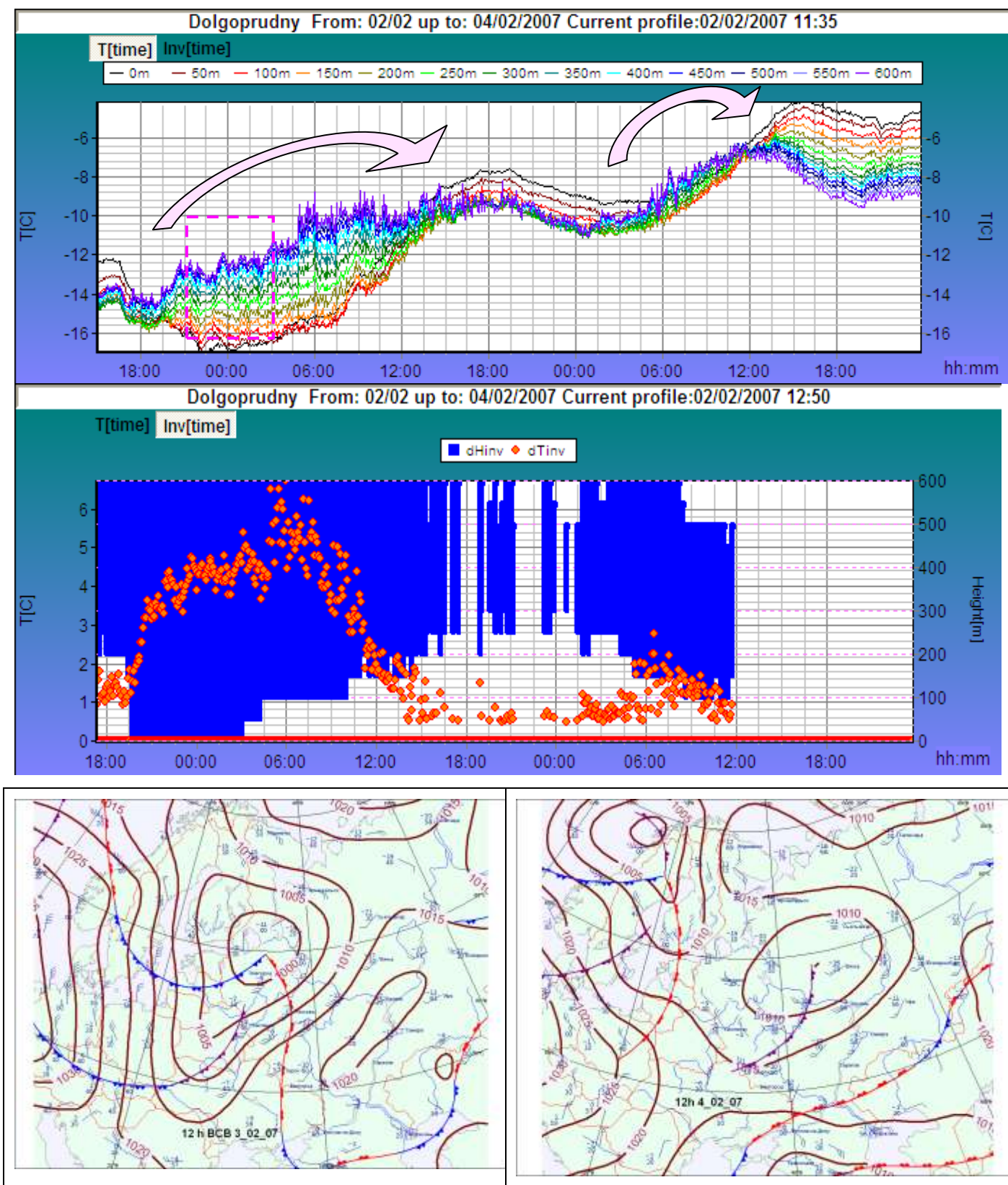


Fig. 5. An example of mixed advection-radiation temperature inversion and weather map for one episode. The first heat wave (the pink arrow in the upper picture) persisted for 12-14 hours with a temperature rise by about  $5^{\circ}\text{C}$  throughout the measurement layer. Against the background of the nighttime temperature increase with low wind the lower inversion boundary descended to the ground due to

cooling (the pink contour in the upper picture). As the turbulent mixing enhanced due to wind increase, the lower inversion boundary rose (below), the magnitude of advection inversion reaching 6 °C - a maximum during the episode described. The second heat wave was less intensive and lasted for about 8 hours, the inversion magnitude being 2°C with the characteristic heights of its lower and upper boundaries of 150 and 550 m, respectively.

In some situations, surface inversion was more than once observed to transform to elevated one, which testifies to an unsteady nature of atmospheric processes - the influence of local mesoscale factors (e.g. the occurrence of jet streams at lower levels) on the thermal structure of the lower atmospheric layers or impeding changes in large-scale processes (e.g. approaching atmospheric fronts, air mass changes, etc.). One should consider such situations as cases of elevated inversion and determine the heights of its lower and upper boundaries as well as its magnitude..

**Note.** If surface inversion is destroyed and transforms to elevated inversion persisting for less than an hour, one can neglect this evolution phase and define inversion duration by the time between surface inversion formation and complete destruction.

### **Mixing layer mean and characteristic heights**

In problems connected with the assessment of weather influence on impurity transport, it is recommended to determine the mean height of a mixing layer for time intervals within a 24-hour period (see 2.1). In establishing an MLH mean, allowing for process persistence, it is advisable to consider times (LT) that are multiples of 3:

- night: 00:00 and 03:00 (00.00 a.m. and 03.00 a.m.)
- morning: 06:00 and 09:00 (06.00 a.m. and 09.00 a.m.)
- daytime: 12:00 and 15:00, (12.00 p.m. and 03.00 p.m.)
- evening: 18:00 and 21:00. (06.00 p.m. and 09.00 p.m.)

In estimating MLH means for 12-hour intervals the times 21:00, 00:00, 03:00, and 06:00 are referred to night periods and 09:00, 12:00, 15:00, and 18:00 to daytime ones.

It is possible to determine MLH more easy: for night in 03.00 a.m., for morning – 09.00 a.m., for day: 03.00 p.m., for evening: 09.00 p.m.

### **3. Analysis of diurnal temperature variation anomalies**

Departures from the normal diurnal temperature variation in the atmospheric boundary layer are indicative of the influence of local factors and changes due to large-scale atmospheric processes, including atmospheric fronts. The normal diurnal temperature variation in the atmospheric boundary layer (ABL) is assumed to be the changing of temperature at measurement levels throughout a 24-hour period,

in a cloudless or nearly cloudless weather with a stationary atmospheric process and weak or moderate speed of transport in the lower atmosphere, i.e. the changing of temperature in the ABL within a thermally uniform air mass without advection and precipitation..

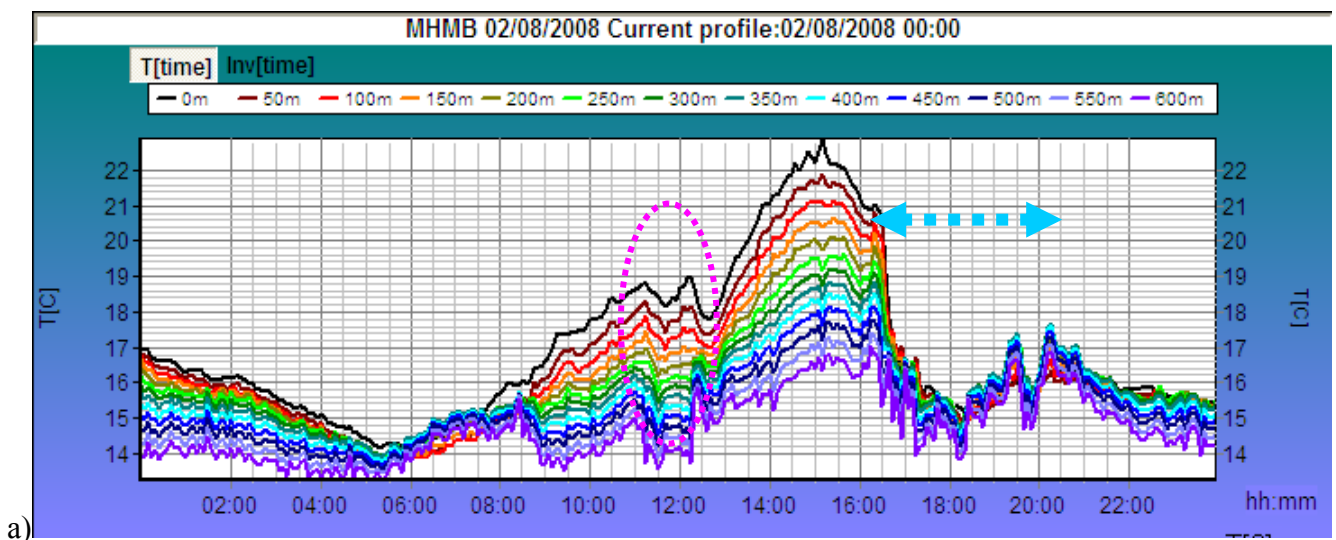
*The typical diurnal temperature variation in the ABL in a warm season* is characterized by temperature steady state at night and unsteady during the daytime. At all the measurement heights, temperature amplitude maximums of 10-15°C and 2-4°C are observed in the surface layer and at 550-600 m, respectively.

*The typical diurnal temperature variation in the ABL in a cold season* differs from that in summer by a lesser amplitude and a longer period of stable stratification. All the deviations from the typical diurnal temperature variation are due to the influence of various factors whose determining is an auxiliary and amplifying means in assessing processes and phenomena that occurred in the previous period.

### 3.1 Passage of a cold atmospheric front

The most dramatic anomalies in diurnal temperature variation are associated with the passage of atmospheric fronts and precipitation. Figures 6 and 7 show temperature changes brought about by a cold front. If a cold front passes during the daytime, vertical thermal gradients in a warm sector ahead of the front are maximal. Most often, 1-2 hours prior to the arrival of a frontal cloud mass, temperature is falling in the surface layer and stops rising in the layer above.

The front passage results in a sharp fall of temperature throughout the measurement layer and frequent short-term temperature oscillations at the upper measurement levels, which is indicative of vertical mixing processes causing colder air parcels from higher tropospheric layers to descend. Within the zone of front, due to mixing, the lower 600-m layer is actually thermally uniform.



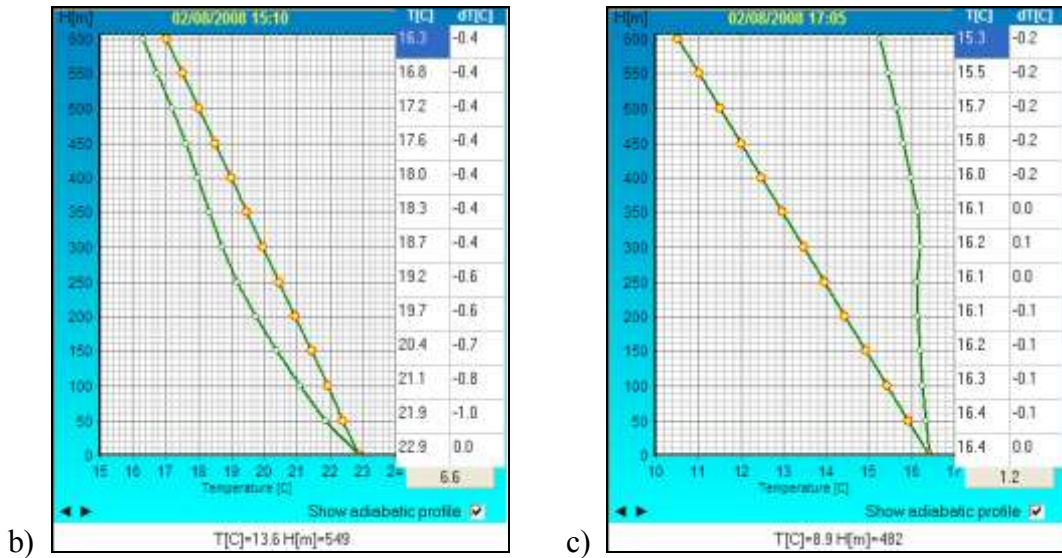
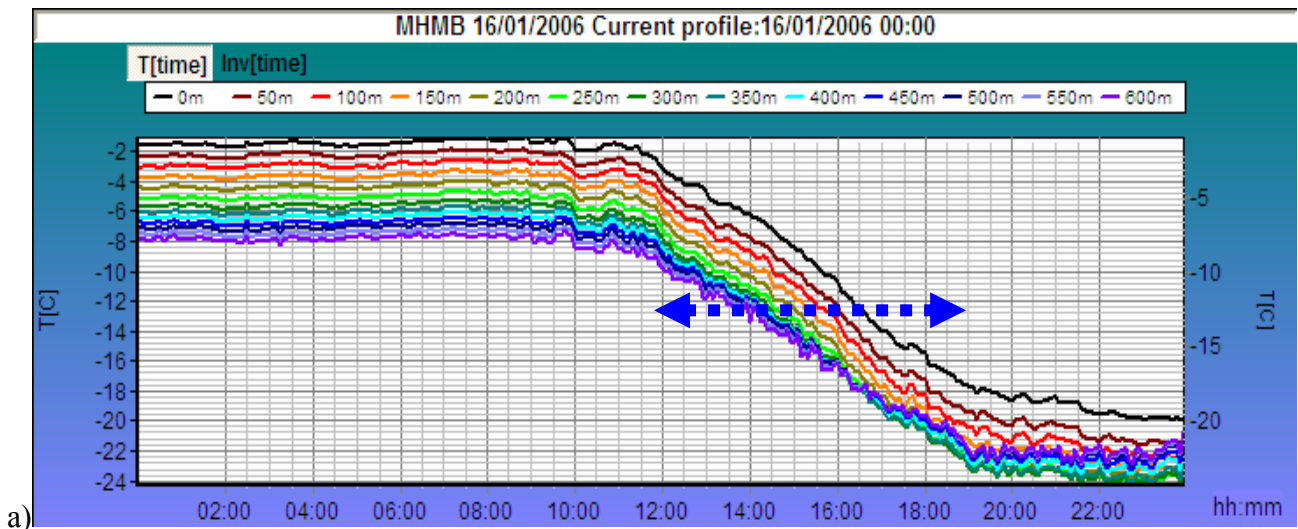


Fig.6.: (a) Passage of a cold atmospheric front in summer (blue arrow, 16:30-21:00); (b) Thermal stratification ahead of the front (highly unstable), and (c) The zone of front (virtually isothermal).

During a warm season, in a warm sector ahead of a cold front, an “instability” zone in clouds, accompanied by wind increase, often forms. In Fig. 6 (within the pink contour in the upper picture) it can be identified by an abnormal for this time of the day sharp temperature rise in the lower layer and temperature oscillations at the upper levels that are due to intensive vertical mixing in a mesoscale vortex

The rear boundary of the frontal zone, i.e. the coming of a new cold air mass, can be established by temperature decrease slowing down or stopping at the upper MTP-5 measurement levels.

The passage of a cold front in winter differed from that in summer by the absence of a zone of intensive convective mixing, the temperature falling simultaneously throughout the measurement layer (Fig. 7) and proceeding to fall until the previous air mass is fully replaced by a new cold one (shown by the arrow). Figures 7a and 7b illustrate cold front passage with vertical temperature gradients in the surface layer preserved or occasionally increased and that with the formation of a nighttime thermal inversion following the front, respectively.



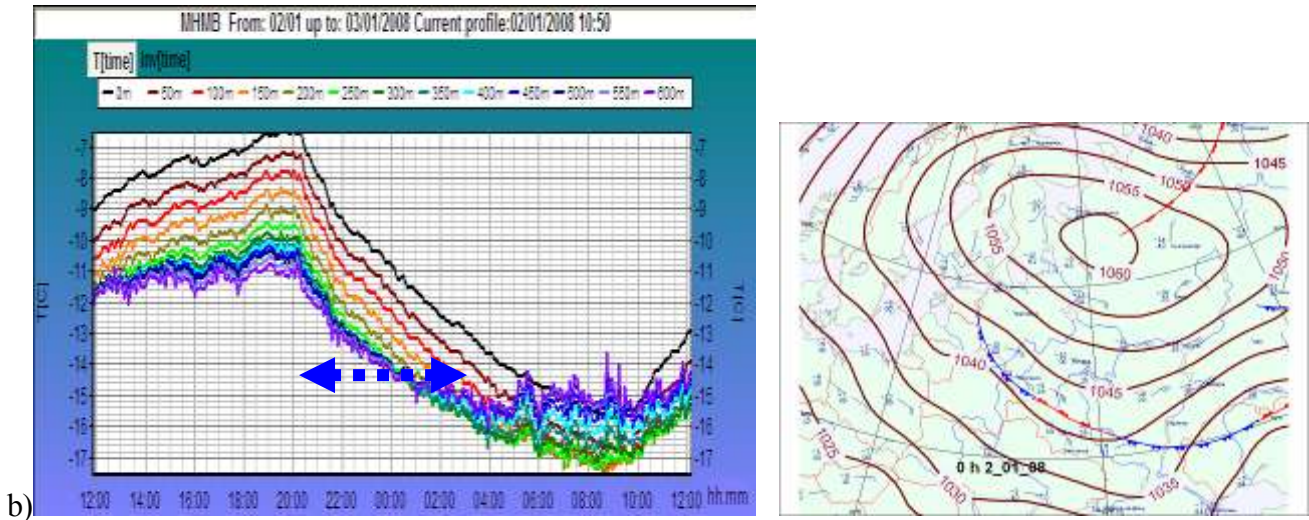
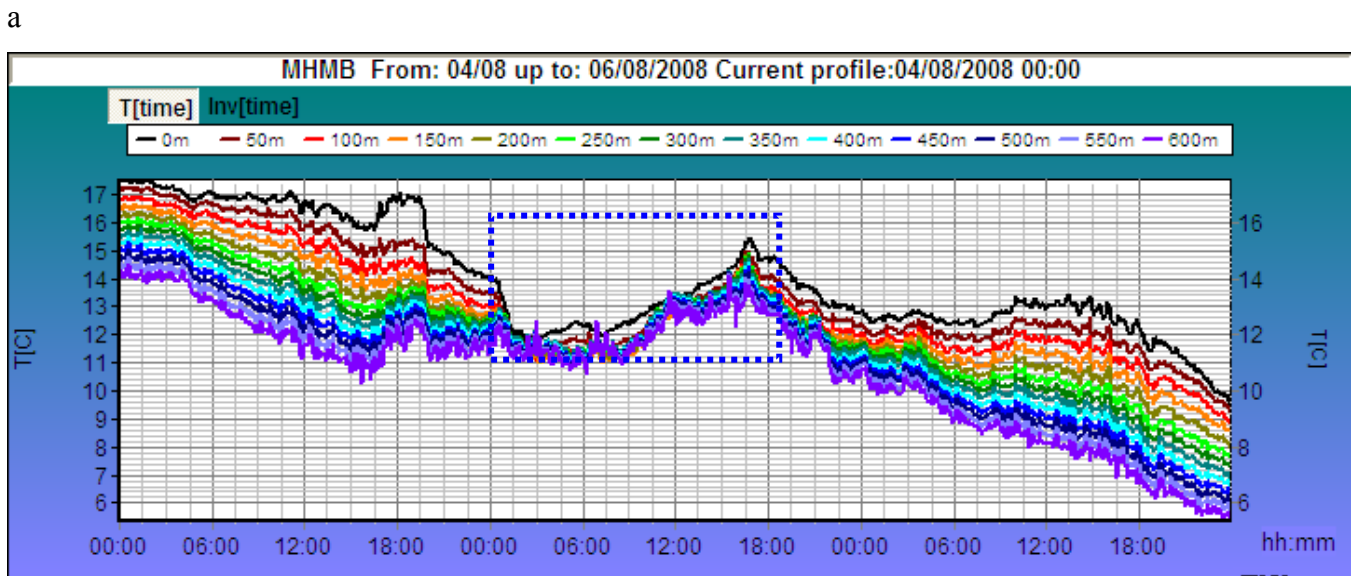


Figure 7. Passage of a cold atmospheric front in winter (a blue arrow).

### 3.2 Secondary cold front

A secondary cold front passage is accompanied by intensive vertical mixing and smoothing out of vertical temperature gradients within the front zone. Figure 8 shows temperature changes in the cyclone rear.



b

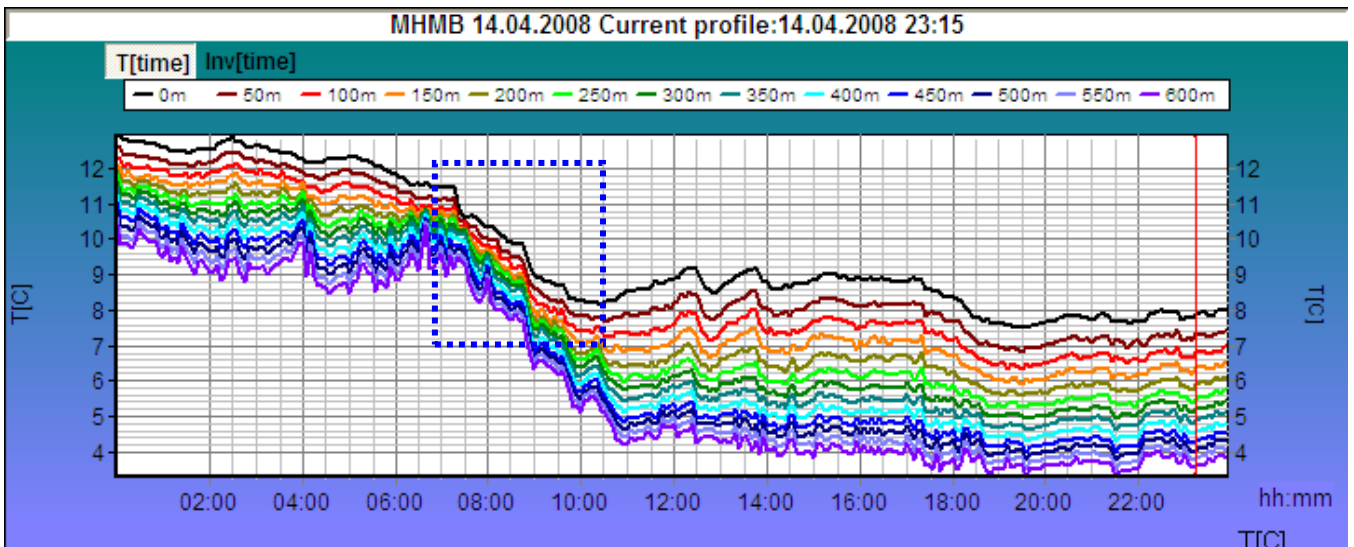


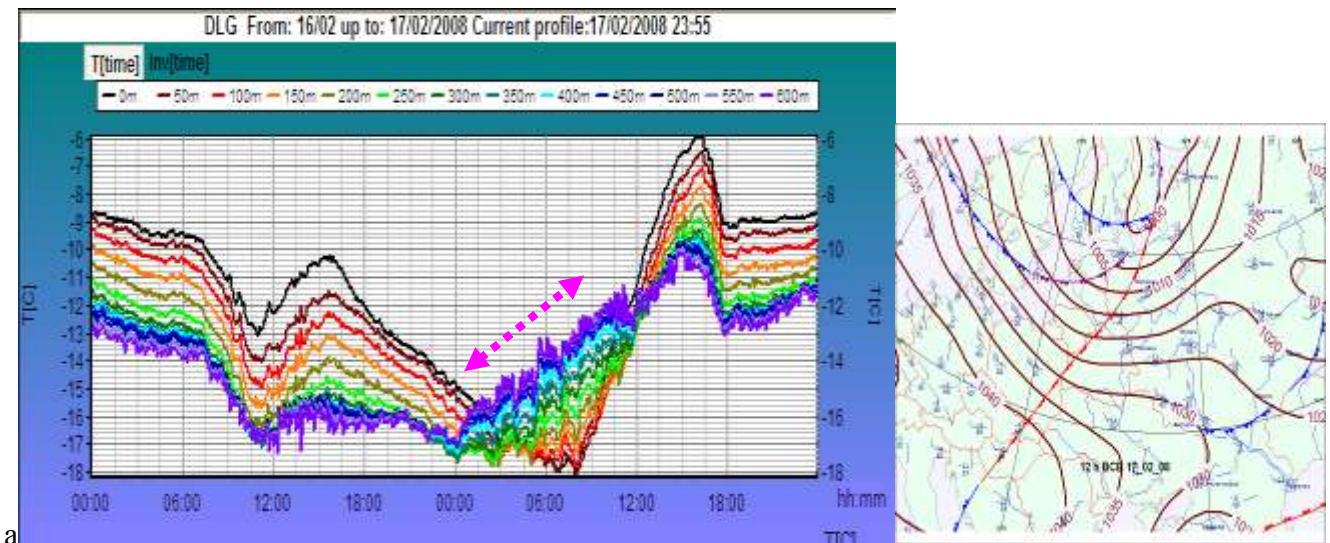
Fig.8. Temperature changes in the zone of a secondary cold front (square contours):

a) in summer and b) in spring.

A secondary front zone is marked by weak thermal stability against the background of unstable stratification prior to the front passage and behind the front.

### 3.3 Warm atmospheric front

An approaching warm front is recognized, based on MTP-5 data, by a temperature rise at the upper measurement heights, which is not due to the daytime heating of the lower atmospheric layers. Figure 9 shows temperature changes in a 600-m layer for warm front episodes in winter and summer.



a

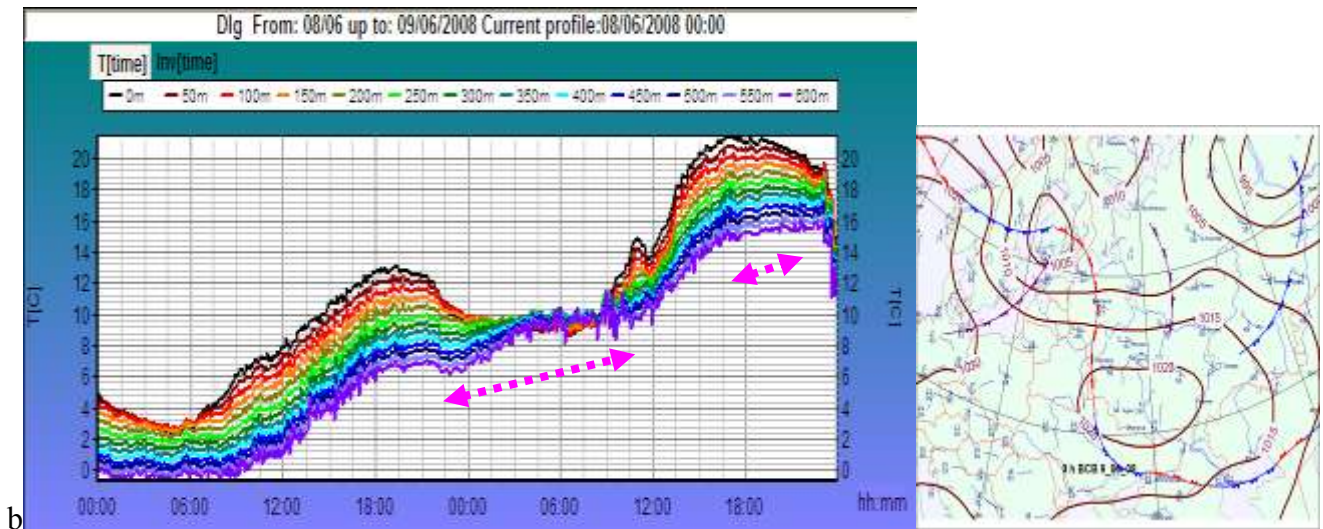


Fig.9. Temperature changes associated with a warm front passage (the pink arrow)

a) *In winter, warm air in the front zone overruns a layer of cold surface air. At nighttime, a mixed temperature inversion is formed: following the front passage, temperature at the surface becomes higher than before, ahead of the front, by 4°C and at 600 m by 6°C.*

b) *In summer, if a warm front passes during the daytime, the temperature within the zone of front is equally increased at all levels,*

*With a warm front passage in the daytime, the temperature in the zone of front is equally increased at all levels, while a nighttime warm front passage is associated with heat advection in the upper portion of the boundary layer ahead of the front, the radiation-advection inversion, however, being much weaker than in winter.*

### 3.4 Diurnal temperature invariability

Diurnal temperature invariability is indicative of a cold air advection, no replacement of the air by a colder air mass occurring during the very first hours, according to surface temperature data. The absence of the diurnal temperature variation may also result from solar radiation deficit due to dense clouds (Fig.10).

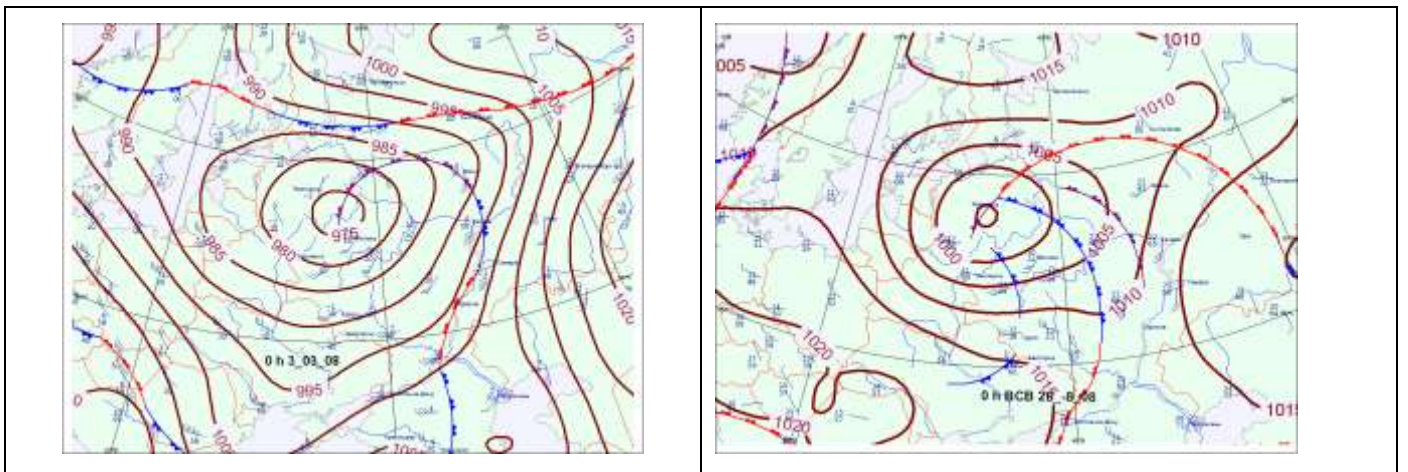
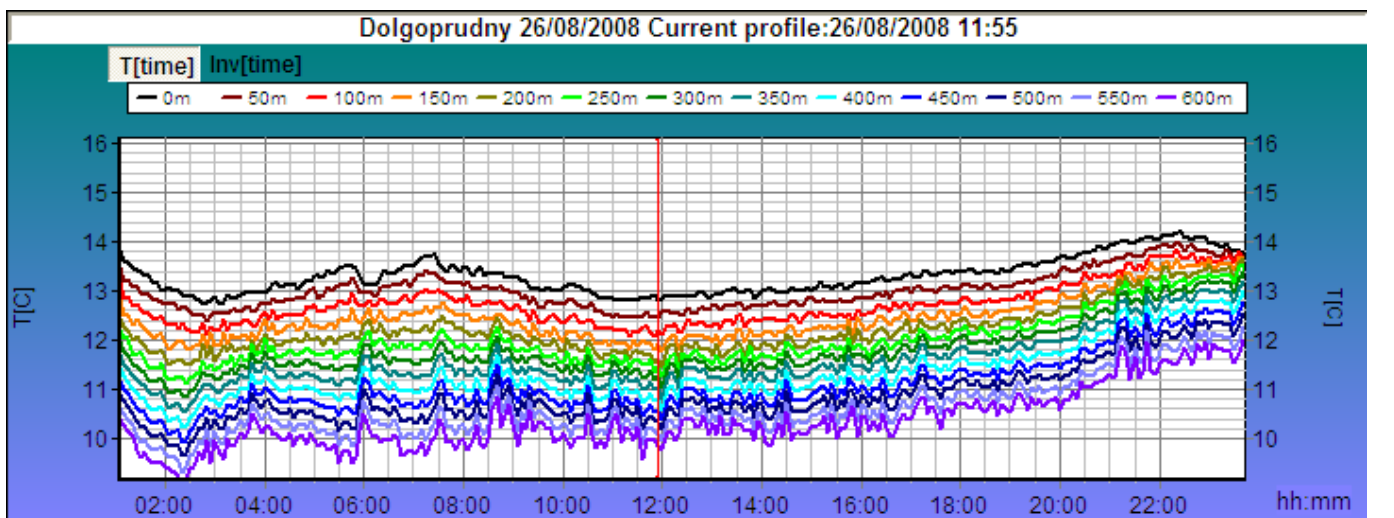
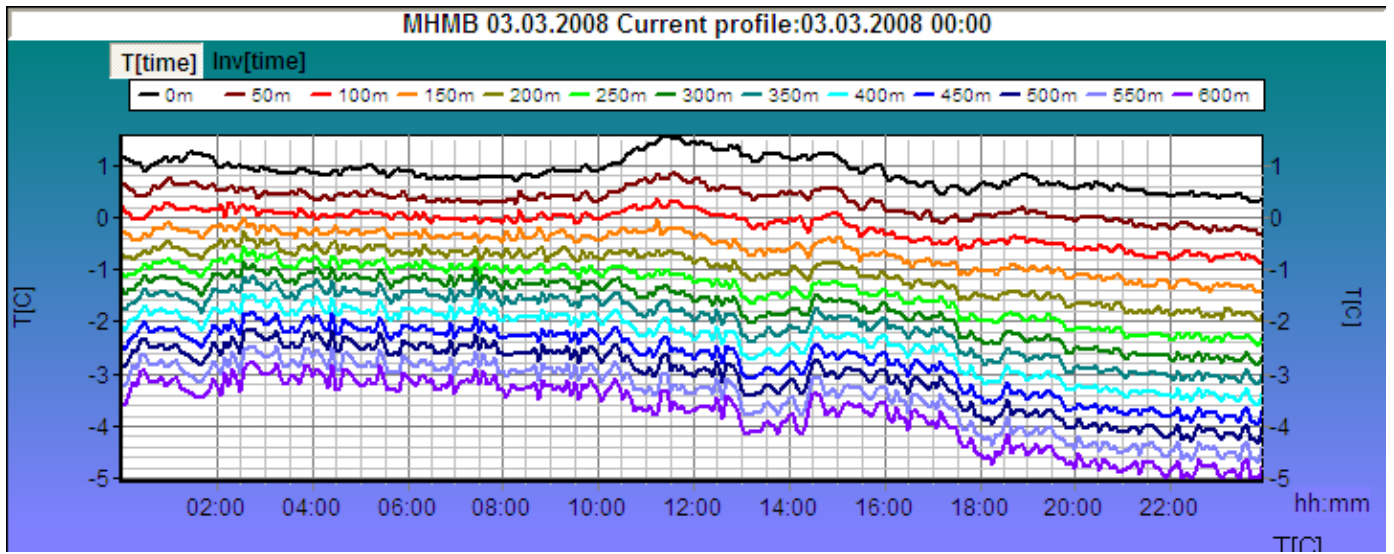
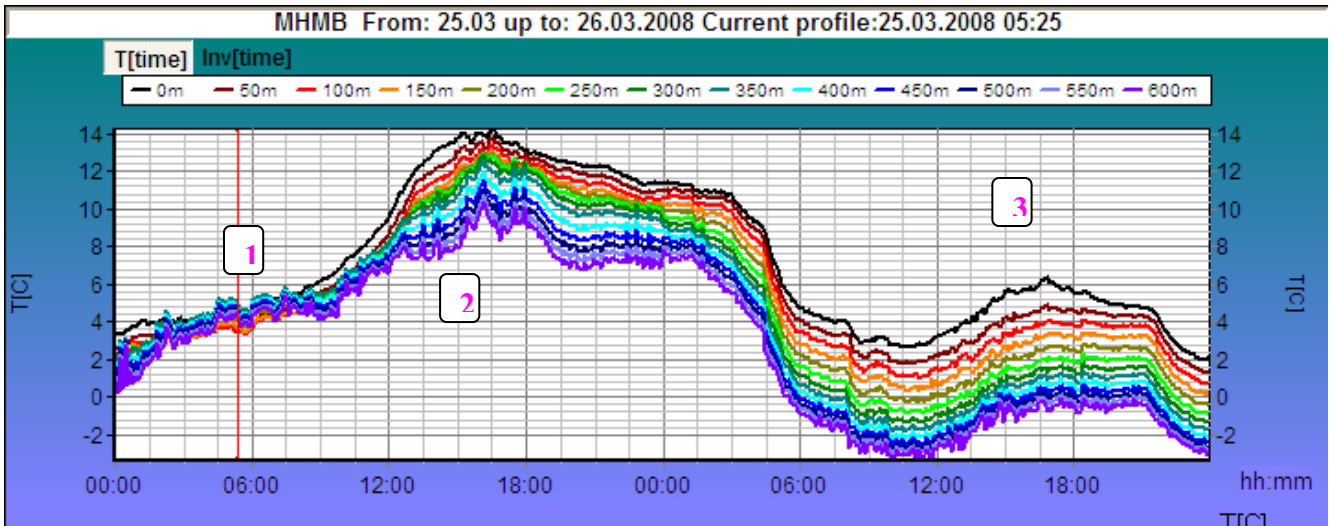


Fig.10. Examples of the absence of diurnal temperature variation during a warm season.

*The absence of diurnal surface temperature variation is accompanied by a temperature decrease at the upper measurement levels: during the period 04:00 – 12.00 temperature at 600 m lowered by 3°C , remaining virtually unchanged at the surface (the upper figure). The figure below shows an abnormal diurnal temperature variation with amplitude of about 1°C in August. Sharp temperature changes at the upper levels are indicative of convective mixing in the layer below the clouds.*

### 3.5 Air mass advection

Air mass advection is always caused by large-scale atmospheric processes and marks the coming of an air mass with other properties and gas composition. The advection of a new air mass is clearly identified from MTP-5 data. In general, immediately after an atmospheric front passage, atmospheric thermal structure in the measurement layer changes abruptly (Fig.11).



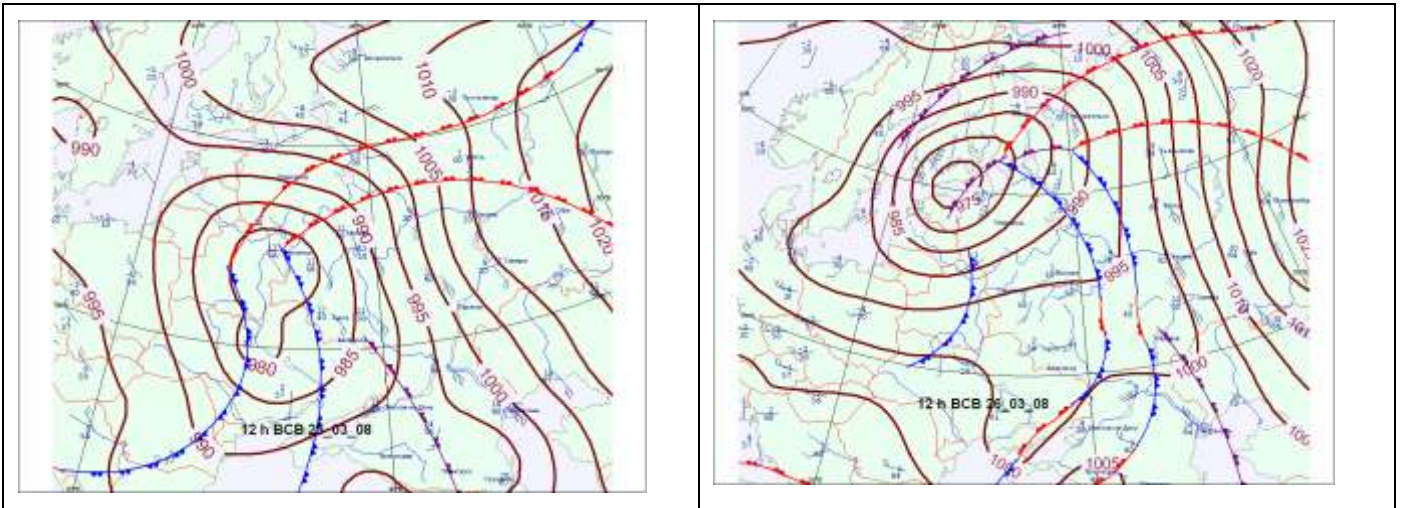
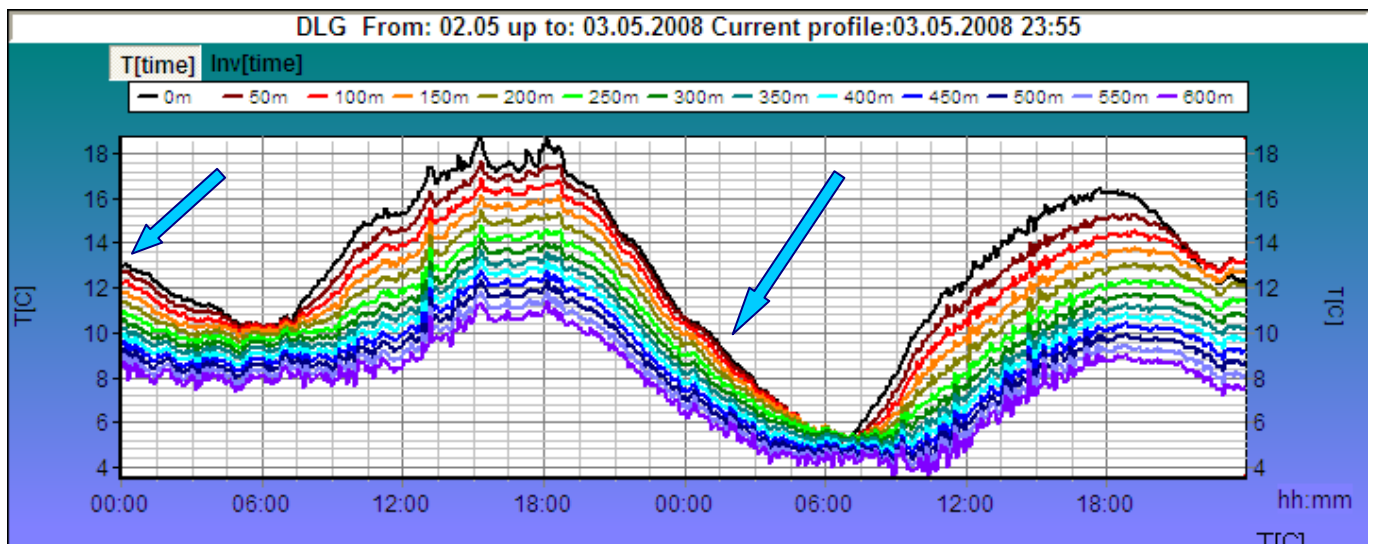


Fig. 11 Thermal state changes in an episode with air mass changing: 1- warming in the zone of front; 2- a warm cyclone sector; 3- thermal instability in the rear of front; the corresponding weather charts.

In some cases with a stationary atmospheric process, most often in an anticyclone or a warm cyclone center, an air mass change occurs in the absence of a pronounced front, i.e., it is not accompanied by cloud amount increase and precipitation. The detection of such phenomena using weather charts and baric topography, with an upper-air observational network being quite sparse, is far from being straightforward. The MTP-5 data analysis helps to reveal air mass changing in such cases. To do this, it is advisable to compare temperatures at the upper levels during similar time periods of the day before. Figure 12 illustrates such a situation.



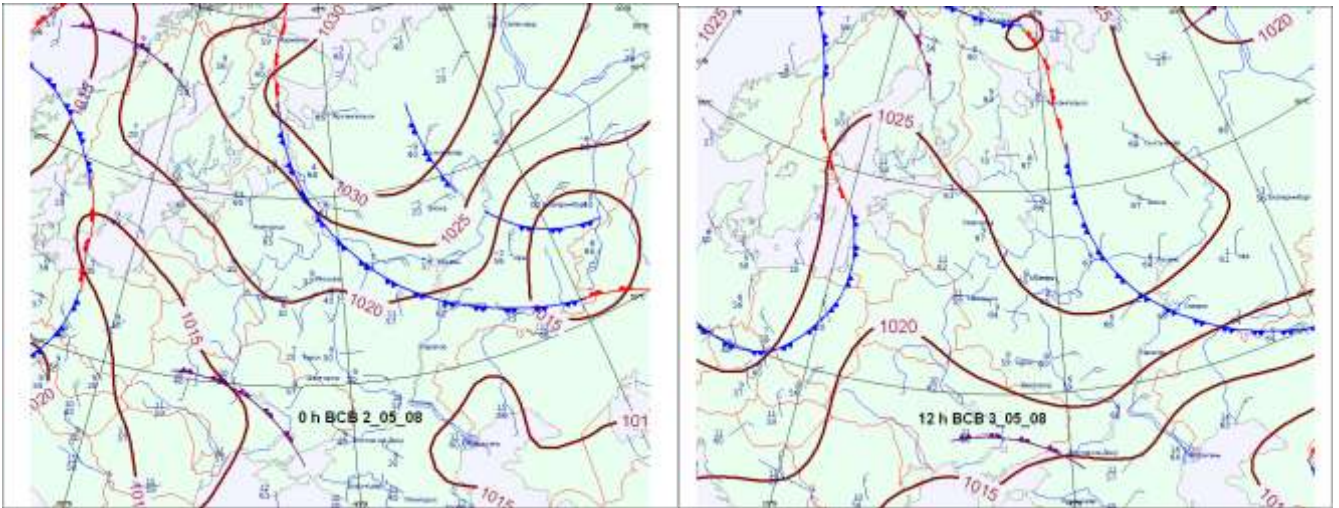


Fig. 12 Air mass changing in a stationary anticyclone without usual signs of an atmospheric front passage (2-3 May) and the corresponding weather charts. *As early as 00:00 on 3 May, air mass changing features showed: the temperature throughout the 600-m layer dropped by 2°C compared with 00:00 on 2 May, and by 06:00 the temperature at the upper levels lowered by 3 °C in comparison with the same hour of the day before. (Note that the maximal surface temperature was also found to have decreased by 3 °C, accordingly.)*

Identification of an air mass change is important for diagnosing meteorological pollution conditions and synoptic predictor description. Thermally different air masses in the same anticyclone must be distinguished, their changes resulting in another gas composition of the lower atmospheric layers. Obviously, an advection constituent must be present in a synoptic predictor.

### 3.6 Variable cloud amount and air-mass precipitation

According to the MTP-5 data, a surface atmosphere thermogram may be either ‘smooth’ or ‘indented’, the latter indicating sharp changes in the solar radiation inflow due to its attenuation by clouds. Figure 13 gives an example of typical temperature changing due to varying cloud amount.

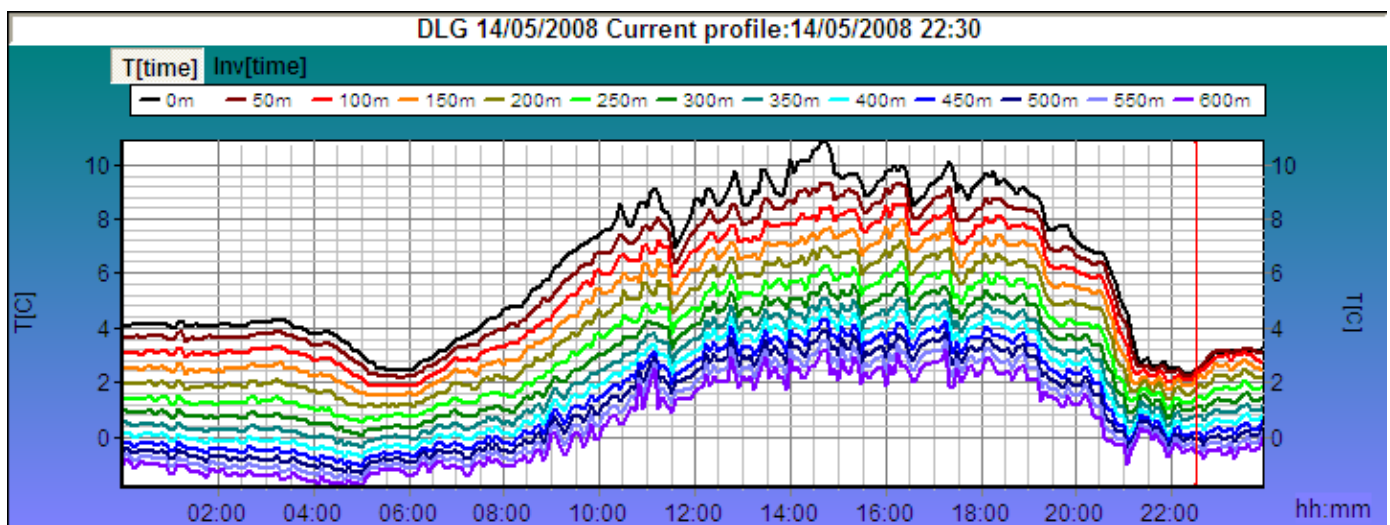


Fig.13 Temperature changes due to varying cloud amount during a warm season.

Short summer rains lead to sharp changes in the thermal structure of the lower atmospheric layers as the boundary layer becomes thermally quasi-uniform due to intensive convective mixing. As convective precipitation stops falling, thermal stratification typical of the current time of the day is generally restored (Fig. 14).

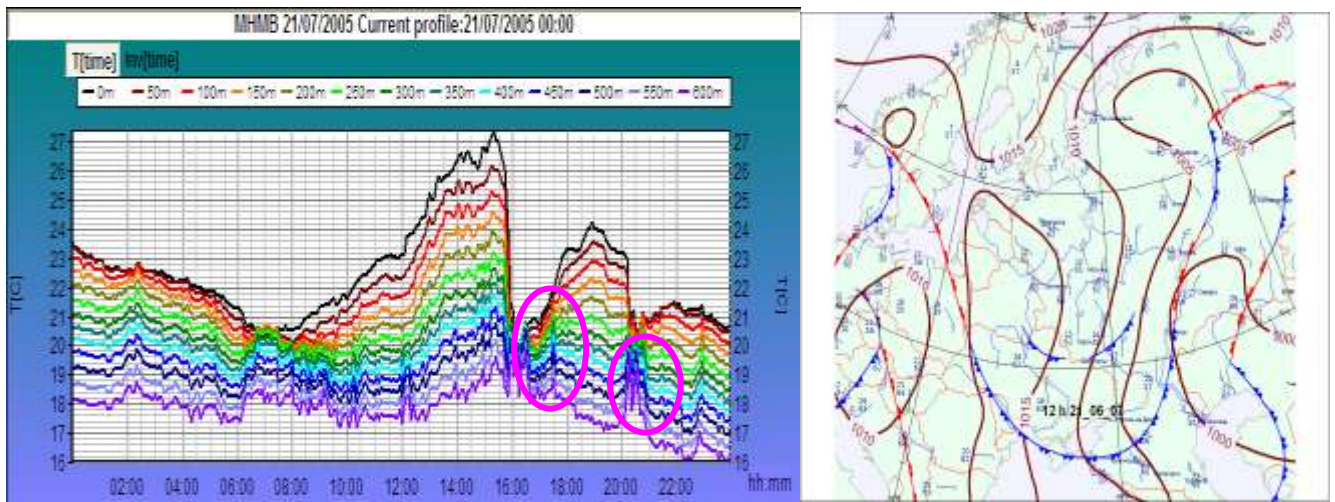


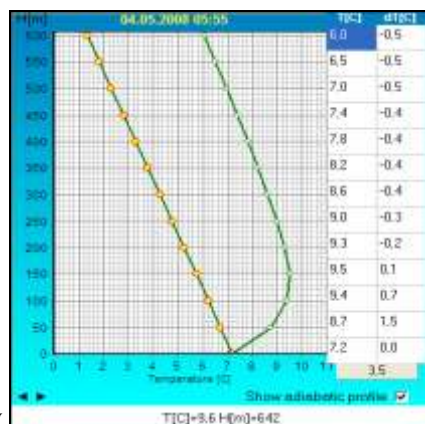
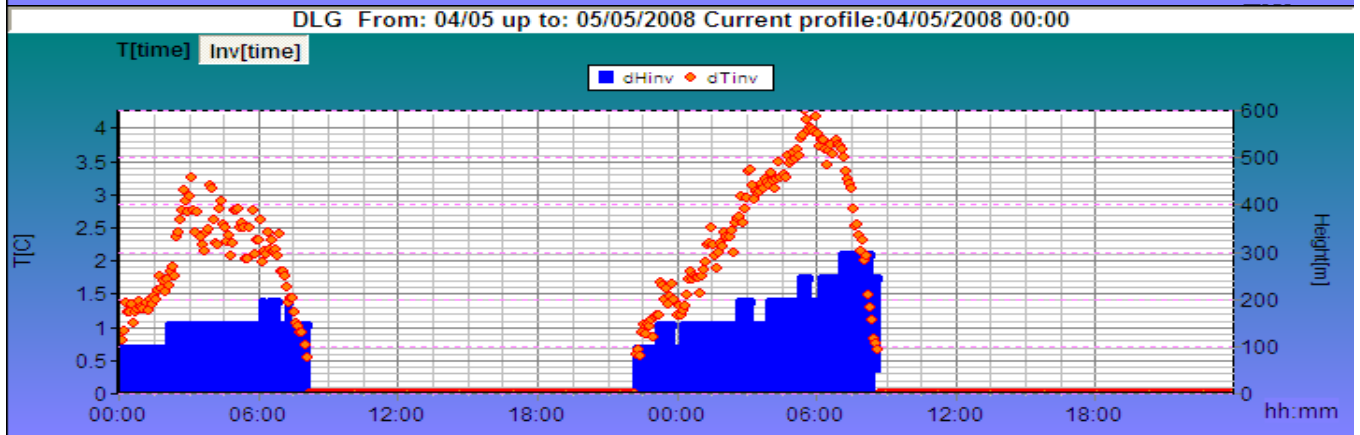
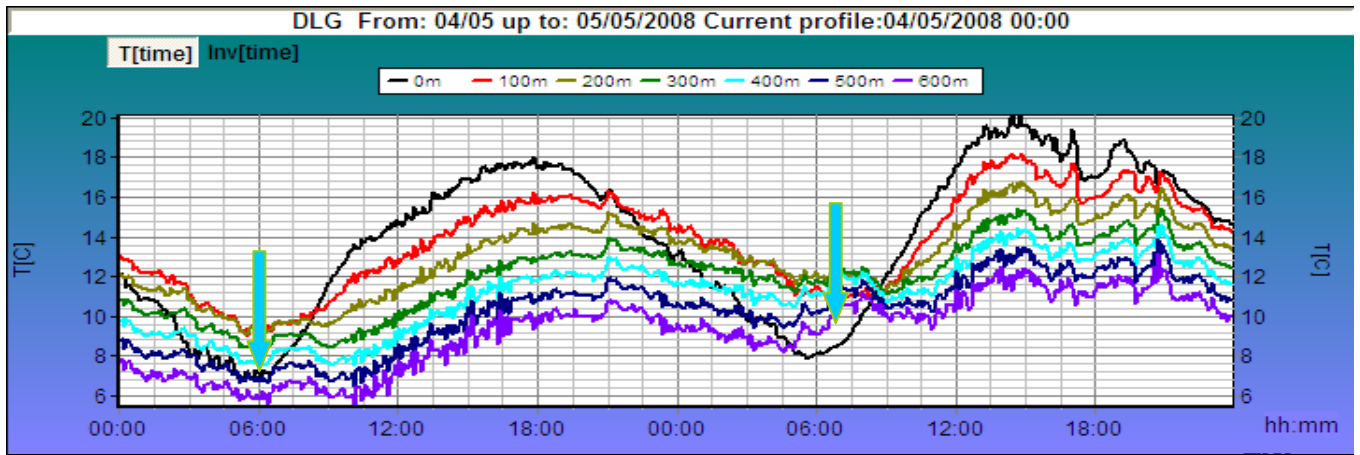
Fig. 14. Thermal structure changes during the rain (pink contours) and the corresponding weather chart. *It rained at about 16:00 and 20:00. Within the interval between the rains, the thermal structure of the lower atmospheric layer was rapidly restored: vertical temperature gradients exceeding a dry-adiabatic gradient were formed.*

During a light rain (with limited washing-out of impurities), a short-term increase of the impurity concentrations can occur as a result of enhanced thermal stability and scattering in the surface layer.

## 4. Temperature inversion

### 4.1 Radiation (surface) temperature inversion

It forms due to underlying surface cooling, generally, with low wind, in a small-gradient baric field or anticyclone. Radiation inversion in unpolluted air forms at sunset and is destroyed 1-2 hours after sunrise. Figure 15 presents temperature changes during a two-day period with nighttime radiation inversions.



4 May



5 May

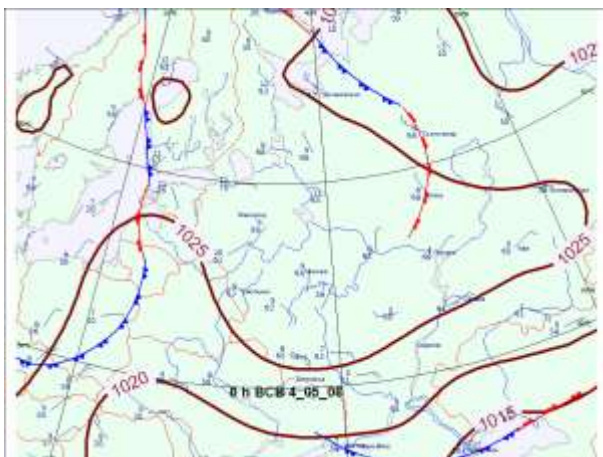


Fig.15. Radiation temperature inversion (from the MTP-5 data): in the thermogram field (the upper picture); visualized inversion characteristics (the middle picture: the inversion magnitude shown by the red line and the inversion layer colored blue); temperature profiles at maximum inversion development

(the pictures below), and weather charts for the episode described (the bottom pictures).

During a stationary atmospheric process (without disturbing factors), inversion enhances from night to night: its magnitude increases and upper boundary rises (Fig. 16).

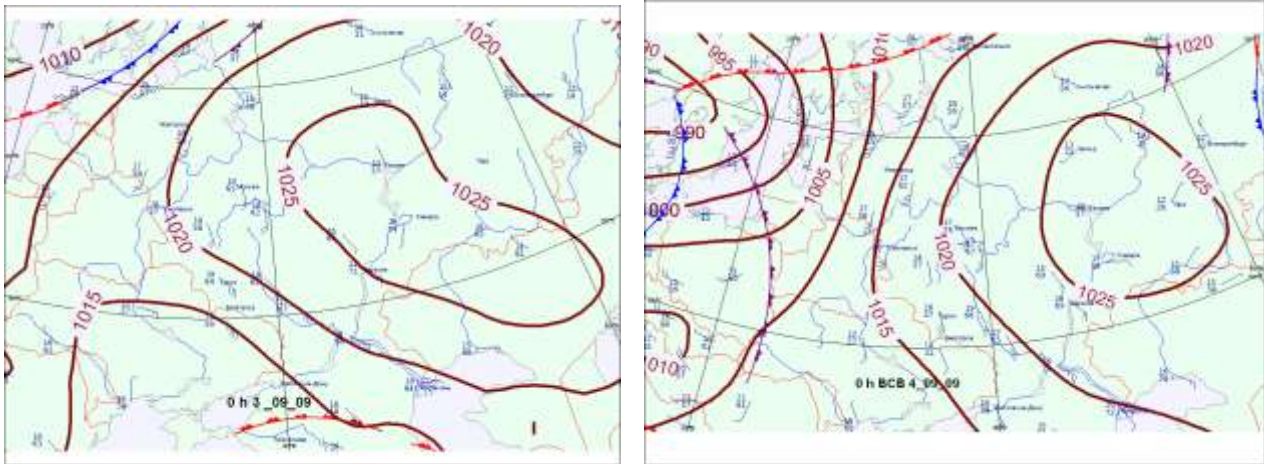


Fig. 16. Radiation inversion enhancement in an anticyclone

#### 4.2 Elevated temperature inversion. Urban inversion

In a warm season, as the sun rises, radiation inversion is destroyed by eddies and transformed to elevated inversion. The process lasts for 1-2 hours. In winter, elevated inversion may persist for a long time from several hours to several days, even without daytime destruction.

Elevated temperature inversion forms:

- in a warm front zone with overrunning warm air ('frontal inversion');
- with a jet-like current in the boundary layer, at maximum speed less than 10 m/s, or with a low-troposphere jet stream ('mesostream') at maximum speed over 12-15 m/s;
- with urban thermal influence on radiation processes; anthropogenic heat makes an effective radiation surface rise above an urban unstable convection surface layer ('urban inversion').

Figure 17 gives an example of temperature time variation in the lower 600-m layer within 3 days, in an episode with the formation of 3 inversion types.

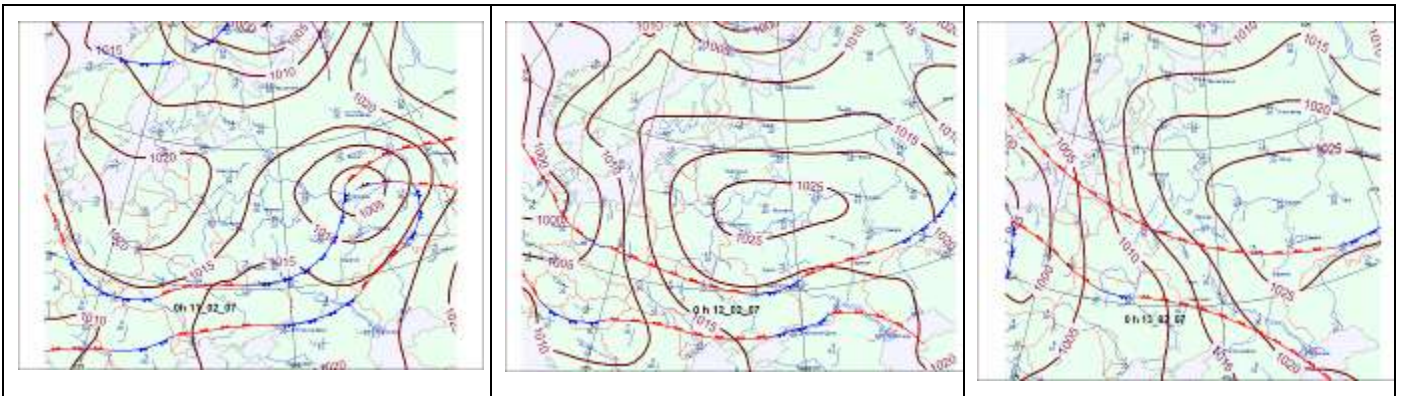
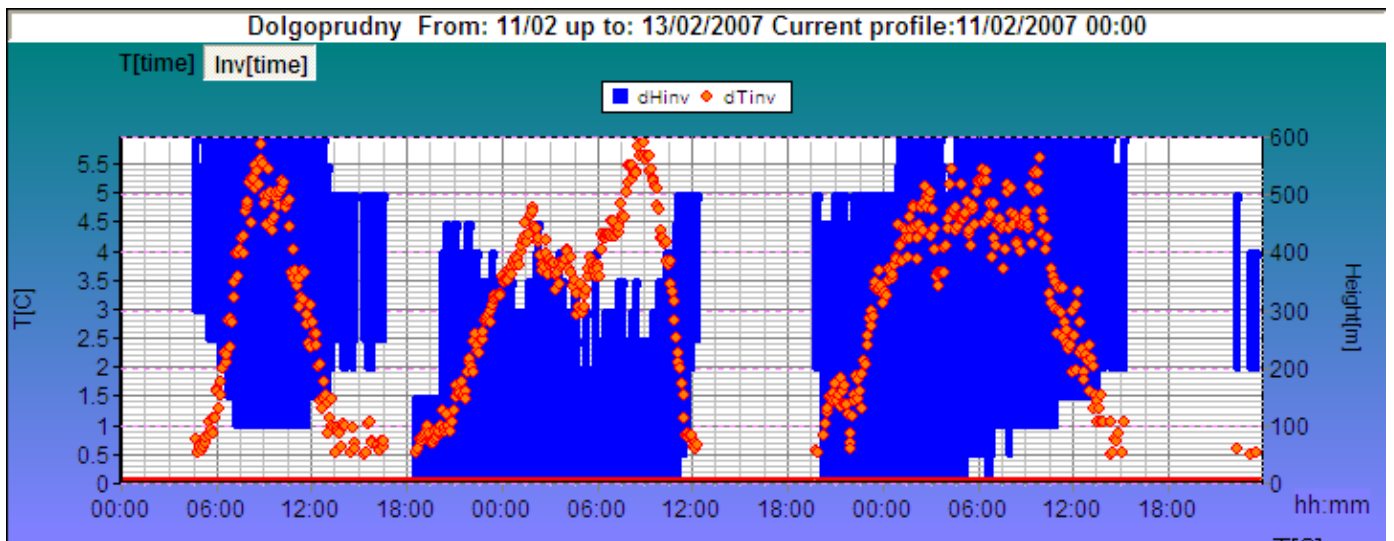
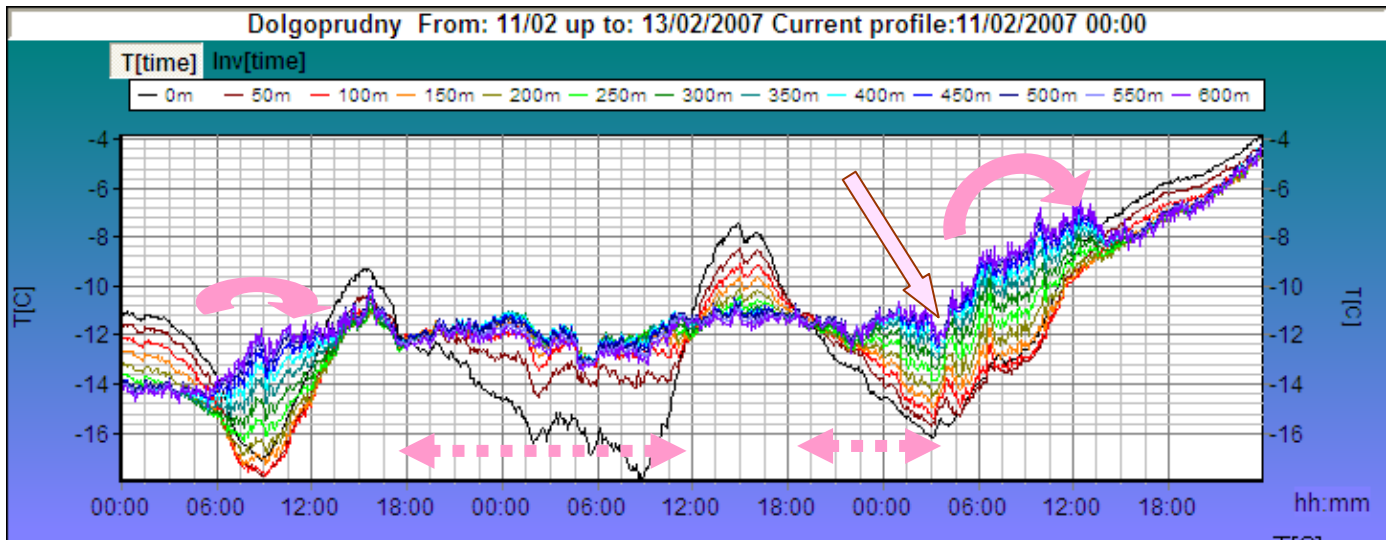


Fig.17. Advection, radiation and mixed-type inversion in a temperature field (the upper picture) and inversion parameters (the middle picture: inversion magnitude shown by the red line, inversion layer colored blue). Initially, in the 11.02 episode, a nighttime advection inversion with turbulent oscillations in the upper measurement layer portion (round arrow) was observed. During the next night, conditions developed that favored underlying surface cooling and surface inversion formation, the latter destroyed at about 11:00 of 12.02. In the evening that day, conditions favorable for cooling were still preserved, and at about 19:00 radiation temperature inversion began to form. In the morning of 13.02, at about

04:00, a new portion of warm air arrived, and surface temperature started rising, proceeding until the end of the day, with advection inversion destroyed at 13:00.

One reason for ‘urban’ elevated inversion development is a direct inflow of heat from a large city. One can judge about the effect from the MTP-5 measurements in the center of Moscow and its environs, presented in Fig. 18.

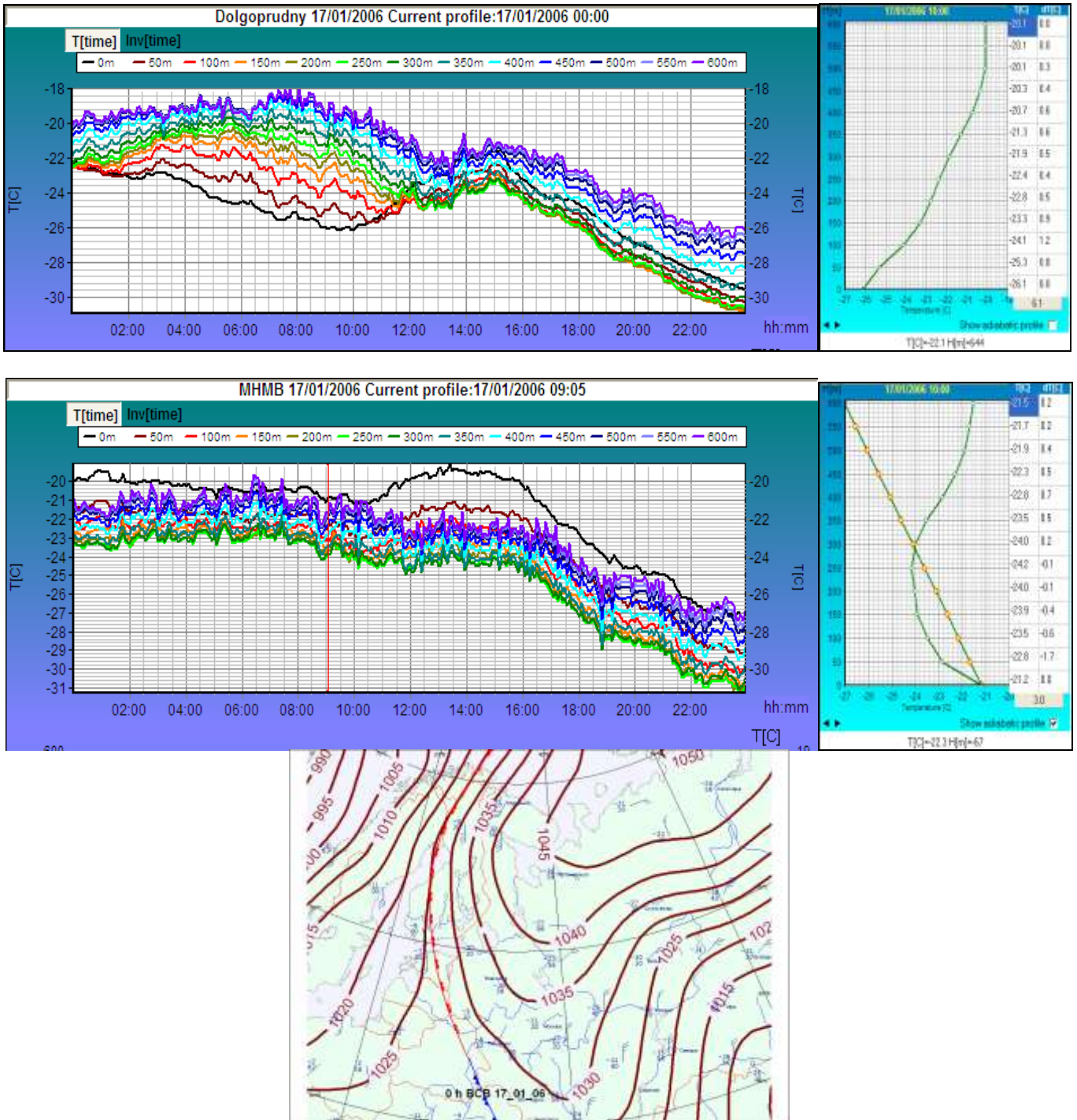


Fig.18. Simultaneous temperature measurements in the lower 600-m layer in Dolgoprudny, north of Moscow (the upper picture) and in Moscow center (below). At night, surface inversion with a maximum

magnitude of 5-6°C developed (the upper profile). In the center of Moscow, conditions favoring convection mixing persisted throughout the night; the lower inversion boundary was at a 300-m level (the lower profile), the inversion magnitude in the measurement layer being about 3°C. The large difference in the thermal structure of the lower atmospheric layer between locations 20 km apart is the result of Moscow thermal influence.

For practical purposes, it is recommended to use thermal stratification observations from both MTP-5 and the nearest radio sounding station. Note that during cold seasons, the man-made influence mainly results from the direct losses of heat from urban heating systems, while during warm seasons, it is the heat accumulated by city buildings and roads that largely affects the thermal structure in the city.

### 4.3 Advection temperature inversion

Advection inversion is a particular case of frontal inversion. It is always accompanied by warm air overrunning colder air and signifies air mass changes (Fig. 19). In warm seasons, heat advection above the boundary layer can only be clearly identified at night as during the daytime, it can be disguised as diurnal temperature variation due to convective mixing.

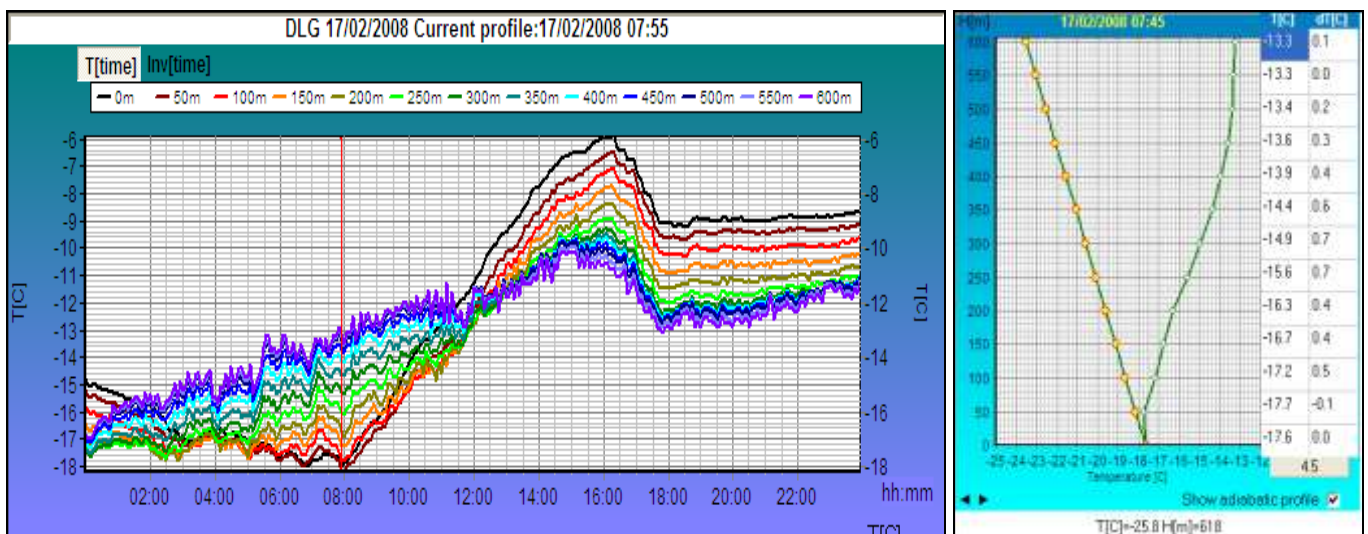


Fig. 19. Frontal (advection) inversion in a warm front (Fig. 9, the chart). As night temperature decreases at the surface, at 600 m it rises: in the period between 00:00 and 08:00: surface temperature dropped by 3°C, while in the upper measurement layer portion, a 4°C increase was observed, the temperature continuing to rise at a 600-m level during the next 10 hours.

Frontal (advection) inversion affects impurity content in the surface layer diversely, the influence depending on the speed of transport, the time of the day and season, advection value, inversion parameters, etc. But, obviously, this influence as a negative factor is basically short-term.

Figure 20 gives a rare example of daytime elevated inversion formation. In this case, synoptic situation was conditioned by a warm sector as an anticyclone's western periphery was being replaced by a cyclone's front part; in the daytime, a lower-level jet stream (LLJS) was traveling over Moscow. The MTP-5 data reported the changing of temperature in the atmospheric boundary layer with the passing of a warm ascending LLJS portion (10:00 – 14:00) and a cold descending one (14:00 – 19:00). While air temperature at 400-600 m was observed to change abruptly by 5-8°C, at the surface there were virtually no signs of intensive mixing that occurred aloft. The inversion described is not a negative factor of surface air pollution either. However, in similar situations during dry periods, dusty air from steppe and desert areas as well as from forest and steppe fires can be transported over large distances.

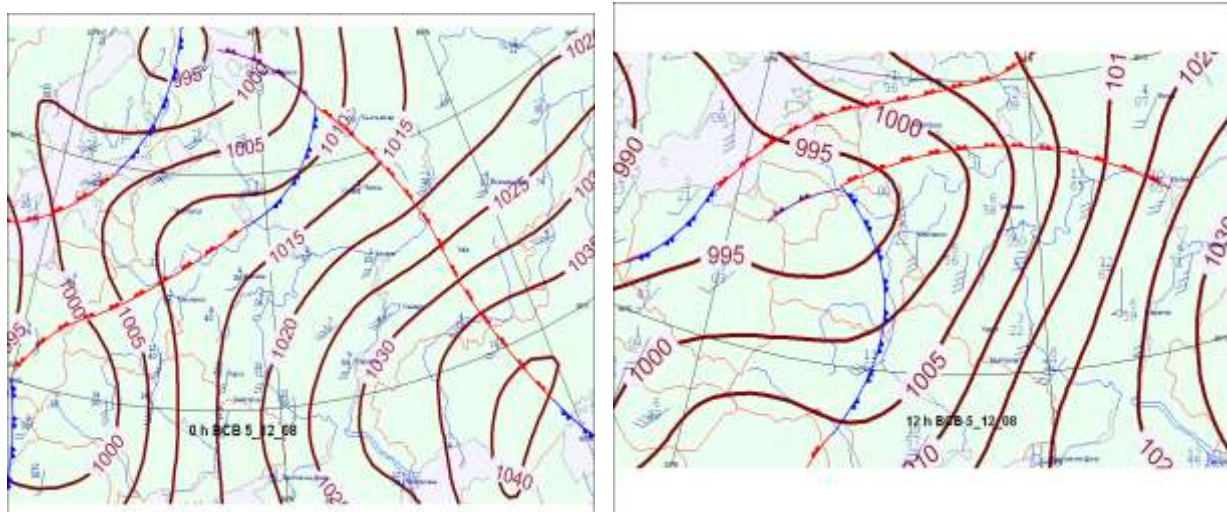
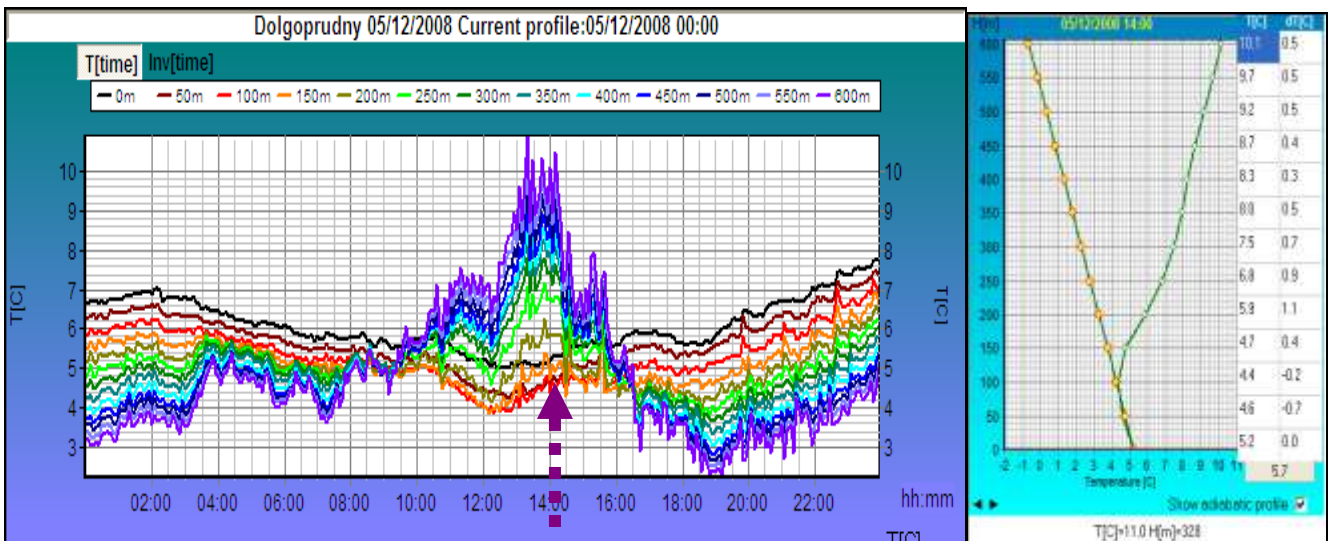


Fig.20. Elevated inversion in a mesoscale jet stream at the lower levels of an occlusion front, in a cyclone's warm sector. *On the right is shown an abnormal daytime temperature profile (inversion at 14:00).*

#### 4.4 Subsidence inversion

This inversion type is due to adiabatic heating of an atmospheric layer with ordered anticyclone downdrafts. Generally, subsidence inversion forms at 1-2-km heights. In an active anticyclone phase, a downdraft effect resulting in enhanced radiation inversion can also be observed in the lower 600-m layer (Fig. 21).

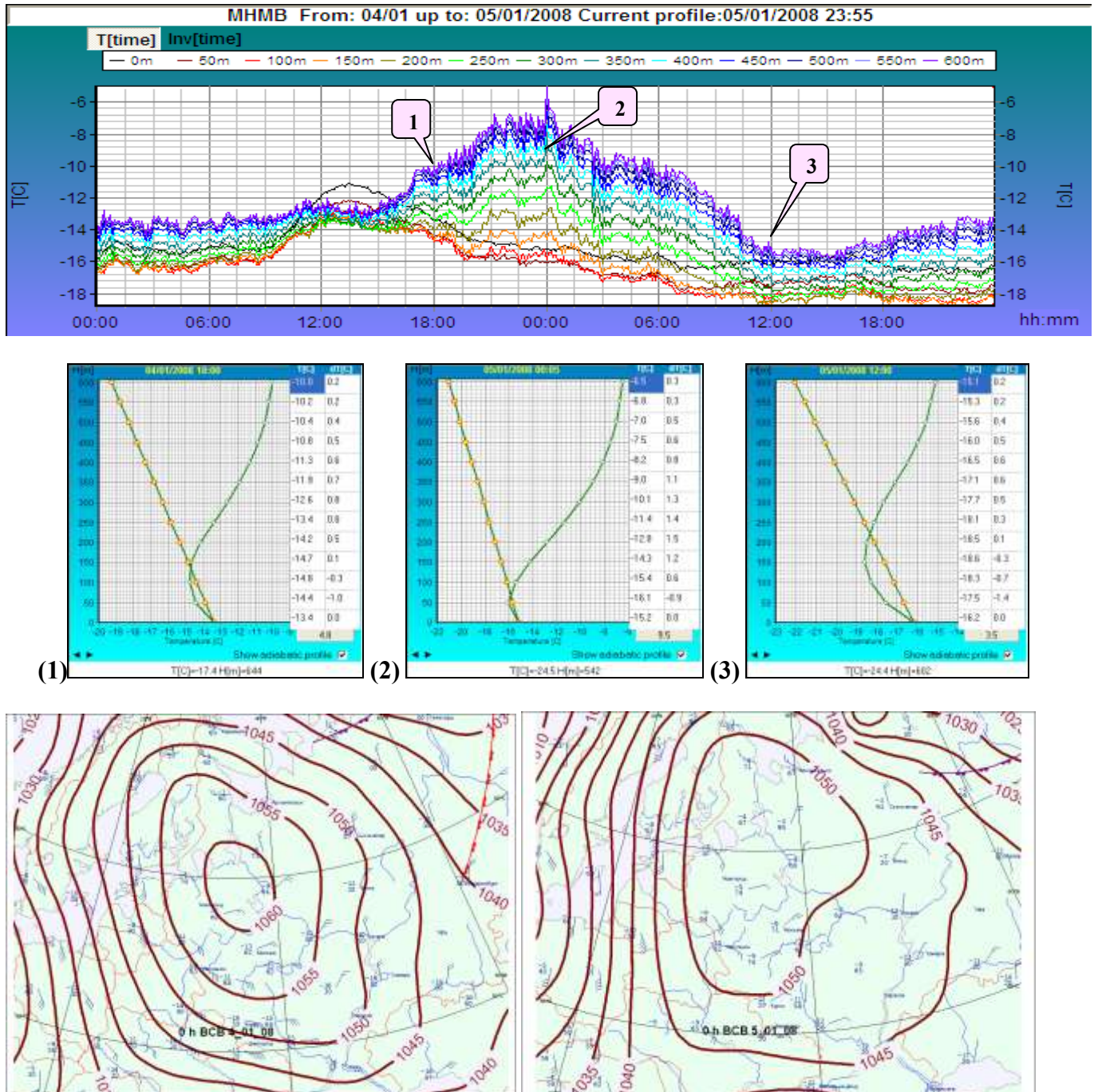


Fig.21. Inversion enhancement due to ordered anticyclone downdrafts.

#### 4.5 Evaporation inversion

Under urban conditions, evaporation inversion can be observed in warm seasons, following afternoon heavy rains. Figure 22 illustrates such an episode.

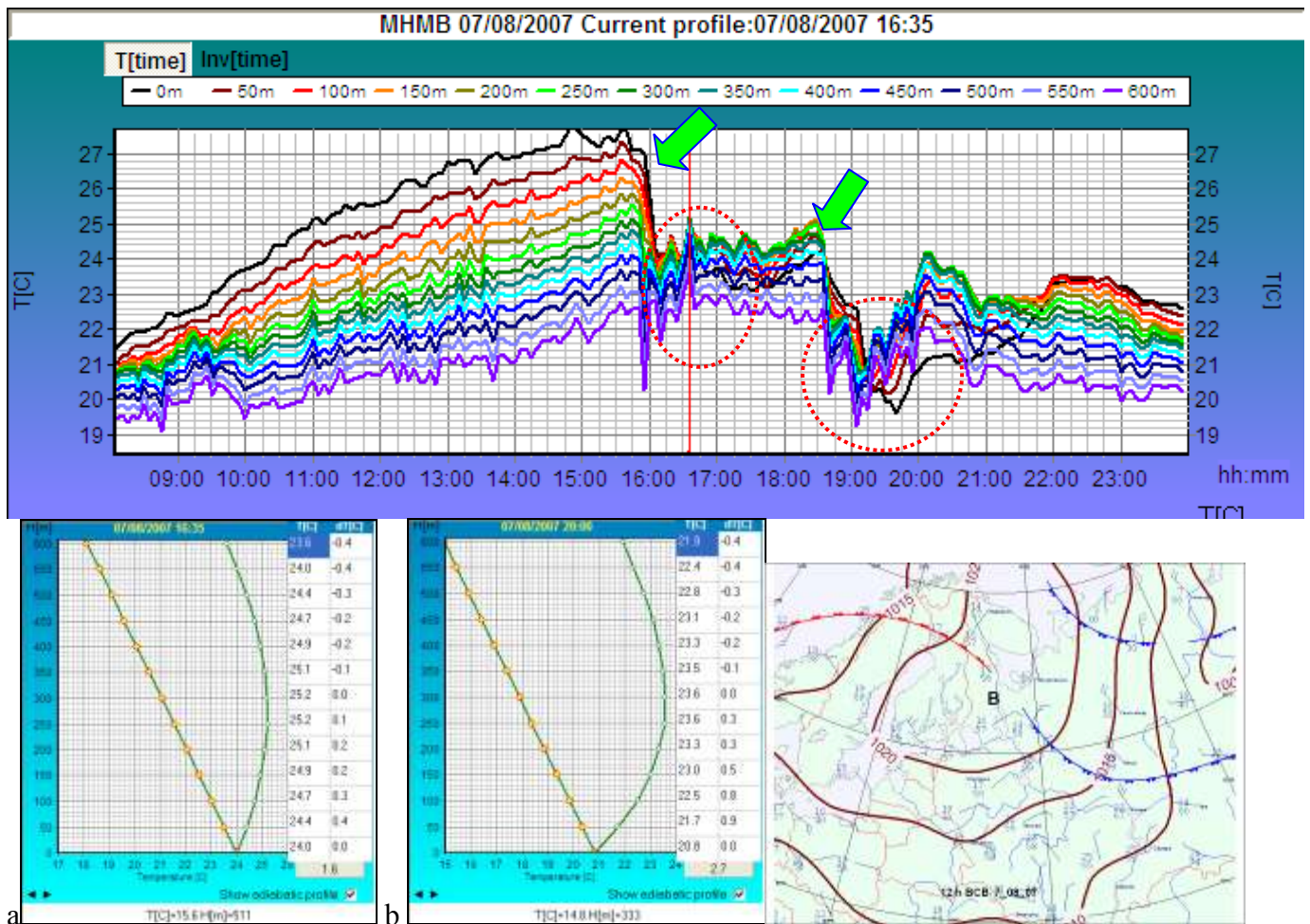


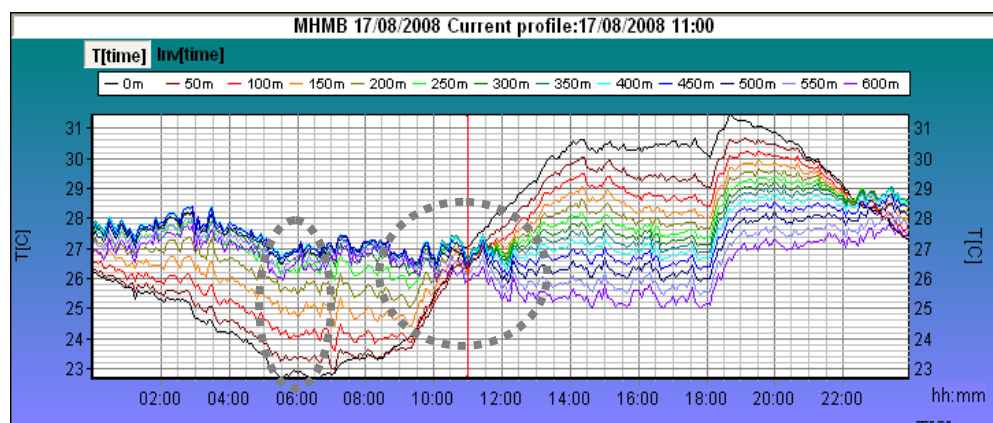
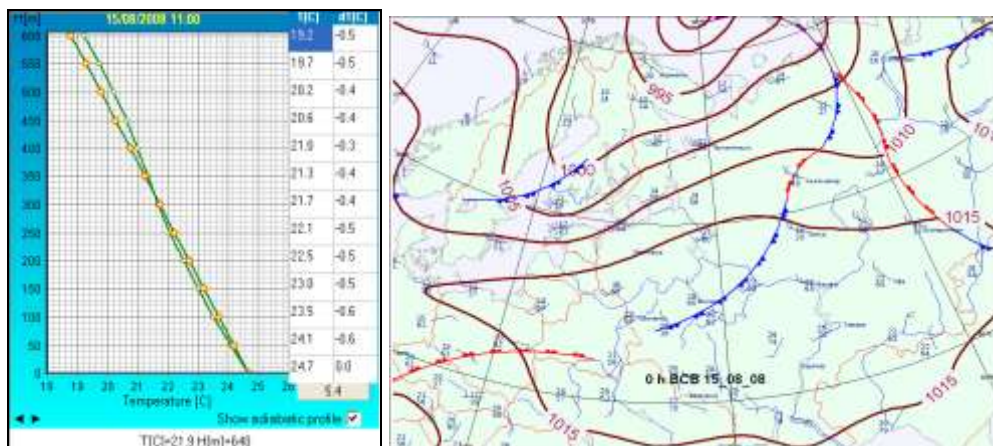
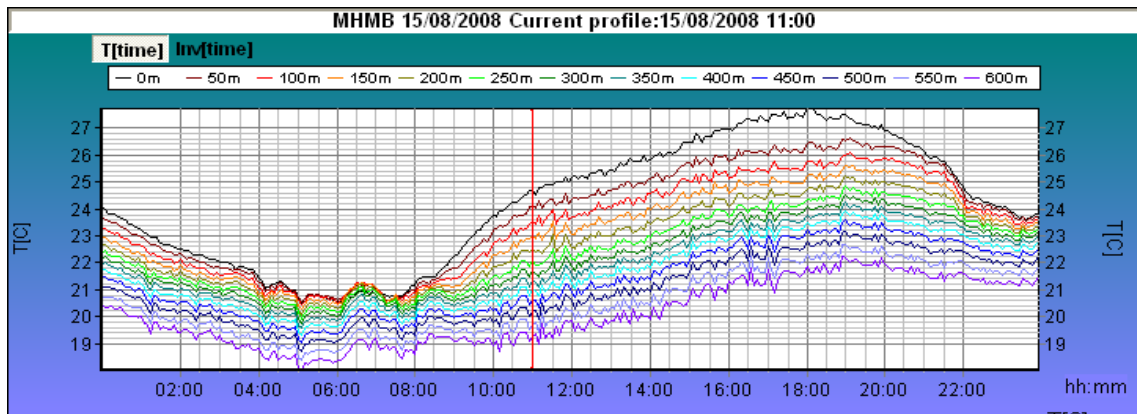
Fig.22 Evaporation inversion (showed by red contours in the top picture) after 7 August daytime shower rain. In the pictures below: temperature inversion a) at 16:35 and b) at 20:00. *The top picture presents two fragments with sharp temperature changes typical of a convective precipitation period (green arrows indicate the beginning of showers). During the first shower, which lasted for less than an hour, the temperature at 600 m changed by nearly 3°C within 10 min., signifying intensive vertical mixing. After the rain, surface inversion formed due to evaporative surface cooling persisted for about 2 hours in an unusual daytime period, its magnitude nearly reaching 2°C. After the second rain, evaporation inversion persisted during the period from 19:00 to 22:00; the nighttime inversion, enhanced by natural cooling, exceeded the daytime one.*

#### 4.6 Aerosol heating inversion

The MTP-5 data make it possible to reveal phenomena caused by the influence of pollutants on thermal processes in the lower atmospheric layers. Enhanced concentrations of greenhouse gases and fine aerosol particles in the lower tropospheric layers lead to the heating of these layers. Two types of

pollution in the lower troposphere are observed – advection and local. Advection pollution is associated with aerosol and gas transport over large distances, from regions with natural fires (forest, steppe, pit, etc.) under conditions favorable for the transport (anticyclone periphery with ordered downdrafts, thermal inversion, the absence of rains, mesoscale low-level jet currents, etc.).

Local pollution is mostly due to urban influences under weather conditions favorable for the accumulation of pollutants. Figure 23 compares two cases: temperature variation in the lower 600-m layer under normal conditions (the picture above) and under weather conditions with intense radiation temperature inversion (the picture below).



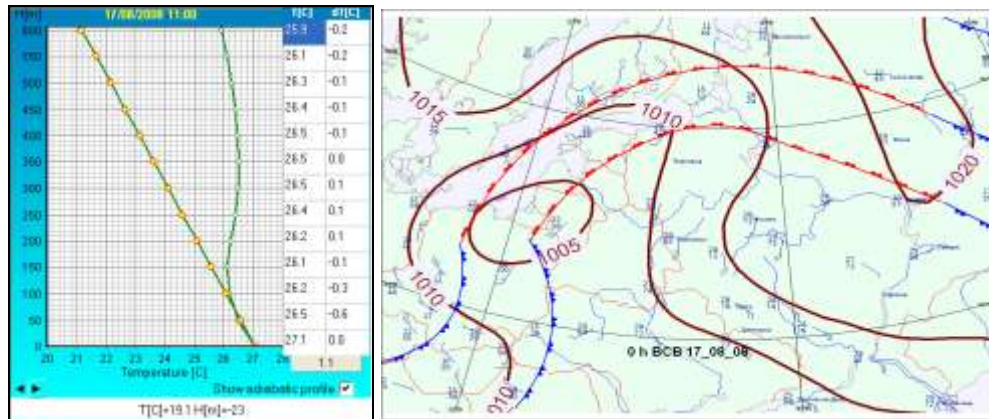


Fig. 23 By 11:00, under conditions of intense mixing usual for morning hours, thermal stratification has approximated to a dry adiabat (above). Under morning weather conditions favoring pollution accumulation, the concentration of pollutants in the lower atmosphere increases, resulting in intense solar radiation absorption, which leads to the heating of the boundary layer interior and hence to thermal stability abnormal for morning hours.

Figure 24 presents an example of polluted air arrival from remote black earth regions registered on the Moscow Pollution Observational Network.

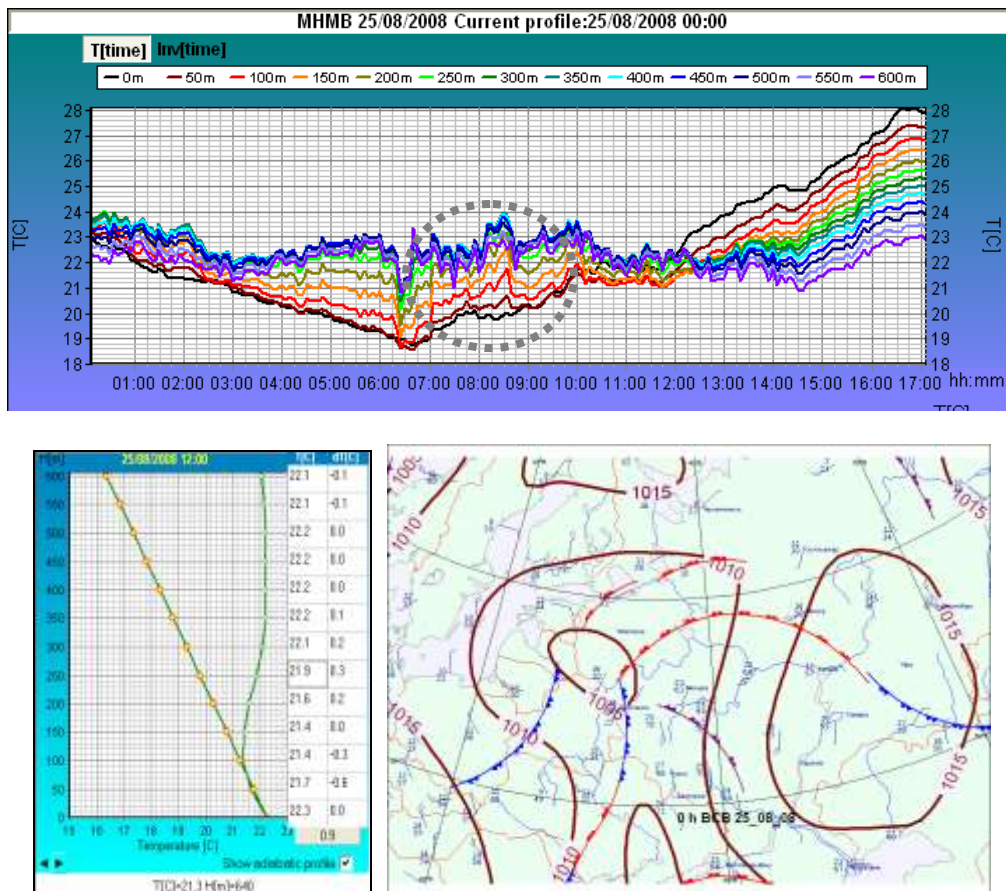


Fig. 24 An abnormal diurnal variation of thermal stratification (grey contour) caused by the advection of polluted air from forest and steppe fires in a warm cyclone sector. August 2008. An abnormally stable

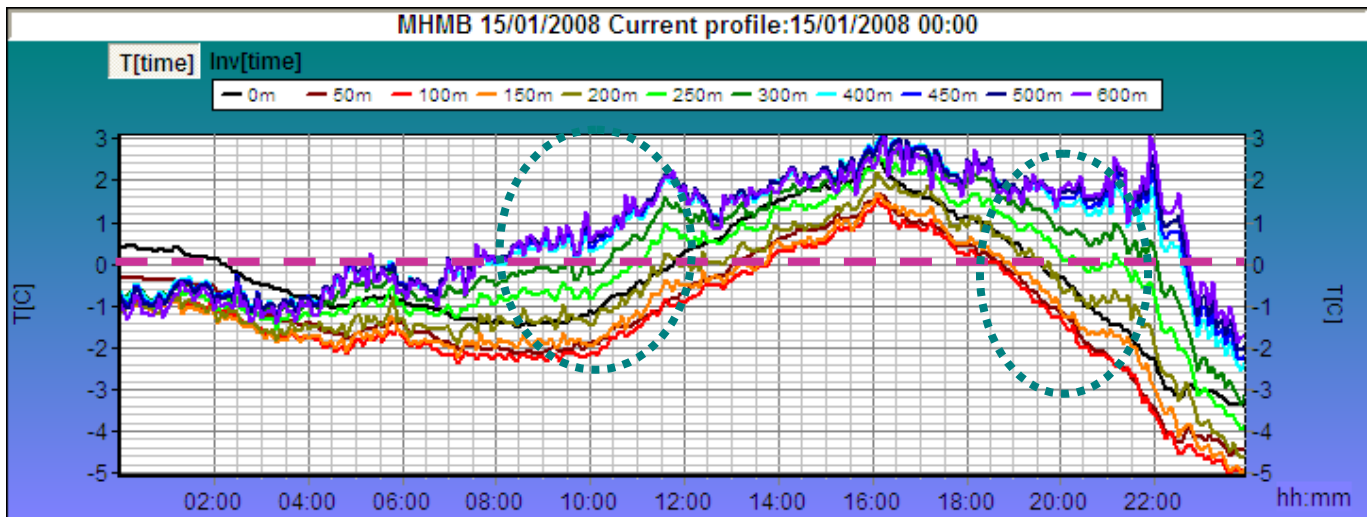
temperature profile (12:00) resulting from the heating of the layer above the surface one, caused by pollutants contained in it, primarily, due to advection (on the right). Sharp temperature changes are indicative of turbulent mixing in the upper portion of the nighttime inversion layer.

Identification of polluted air arrival from other regions by abnormal 24-hour temperature changes in the MPT-5 measurement layer is of importance in understanding the reasons for enhanced urban pollution and hence in the relevant decision-making.

## 5. Identification of icing thermal conditions

This hazardous natural phenomenon is associated with warm air advection in periods with temperatures decreasing to below 0°C. With information about the thermal state of the lower atmospheric layers being scarce, MTP-5 data enables an early assessment and observation of the process of warm air (with temperatures above 0°C) overrunning the surface layer with negative temperatures, as well as determining precipitation phase (liquid, mixed or solid).

Figure 25 illustrates an episode with the thermal state of the lower 600-m layer under conditions occasionally leading to icing.



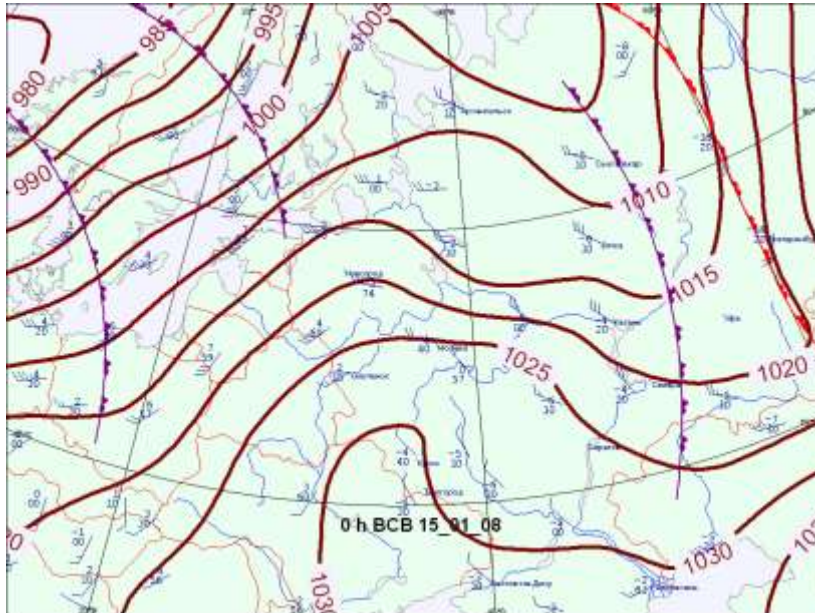


Fig. 25 Icing conditions (blue contour): during 08:00 - 12:00 and 19:00 - 22:00 periods, the temperature in the surface layer is below 0°C, while in the layer above (300-600m) it is above 0°C. During a 14:00 – 18:00 period, the conditions are favorable for liquid precipitation formation. (Dashed line indicates 0°C).

## 6. The use of MTP-5 data in analyzing and forecasting meteorological pollution accumulation conditions

An early prediction of heavy pollution episodes is one of the major problems in air quality forecasting. Such episodes (except anthropogenic emergency situations) are preceded by specific conditions in the lower troposphere; in most cities, a light wind in the lower boundary layer portion with stable stratification persisting for not less than 3-6 hours is a precursor.

The statistical air pollution forecasting schemes employed by Roshydromet comprise meteorological parameters including a so-called ‘synoptic predictor’. In making forecasts it is important to correctly diagnose the current state of the lower atmosphere and appreciate the preceding processes, including the nature of observed temperature inversions.

Observations using the MTP-5 instrument permit diagnosing one of the major elements of unfavorable weather conditions – thermal stratification. The physical processes associated with scattering are universal, but due to local physiographic features and particular pollution sources typical of each city, episodes with weather conditions leading to high pollution concentrations are brought about by different factors. To reveal them, it is necessary to establish thermal stratification characteristics favoring hazardous accumulation of pollutants.

The basic approach to follows in analyzing MTP-5 data aimed at identifying meteorological pollution accumulation conditions builds upon establishing the intensity of mixing and air changing, i.e. atmospheric processes leading to pollution removal from the surface layer. Undoubtedly, MTP-5 data

analysis must allow for the speed of transport in the lower atmospheric layers. According to observations carried out in Moscow, pollution concentrations in the surface air are not high if an average speed of transport in the lower layer up to a 925 hPa isobaric surface is over 6 m/s. A particular 'critical' average speed of transport in each city is a measure of the probability of pollution accumulation conditions in both diagnosis and prognostic periods. In the operational diagnosing and forecasting of meteorological conditions leading to pollution dissipation it is recommended to fulfill the analysis in the following order, providing visualization of MTP-5 data for the preceding and the current 24-hour periods:

**a. Assess atmospheric process stationary conditions for each diagnosis and forecast period by establishing whether**

- an air mass change occurred within the last 6-12 hours (the period long enough for air pollution to reach a critical value and specific to a particular city);
- air advection with considerable temperature changes (not less than 3°C in a warm season and not less than 2°C in a cold season) is observed;
- heavy or moderate precipitation occurred within the last 6-12 hours.

*The absence of the above factors is enough to signify the absence of pollution accumulation conditions during the diagnosed and the following prognostic period.*

**b. Determine the origin of temperature inversion (if any) in the preceding period**

- taking into account that advection inversion is indicative of an air mass change, while radiation inversion, if developed without external forcing, signifies the presence of preconditions for pollution accumulation in the surface layer;
- judging by the form of thermograms during inversion periods about the presence of external forcing which reveals itself in sharp temperature changes and can be indicative of the presence of a jet stream, large wind shifts, a disguised air mass change, enhanced turbulent mixing, etc.

*Figure 26 shows examples of radiation inversion in the absence of turbulent mixing in the inversion layer, disturbed by the motion of the lower-level jet stream. As can be seen from the picture below, at about 09:00 (the time of making a forecast of meteorological conditions favoring pollution accumulation), quantitative inversion characteristics are essentially the same in both examples. The picture on the right illustrates a short-term thermal instability due to the lowering of a meso-scale jet stream (at about 01:00) during about 5 hours contributing to air mixing in the inversion layer.*

- estimating the inversion and mixing layer characteristics (if they are included in the scheme of pollution forecast as a persistence factor), taking note of whether the actual time of inversion formation and destruction coincides with mean seasonal characteristics. Considerable time shifts (e.g. late inversion

formation and destruction) may signify an increase in urban air pollution in the absence of any signs of influence by other factors.

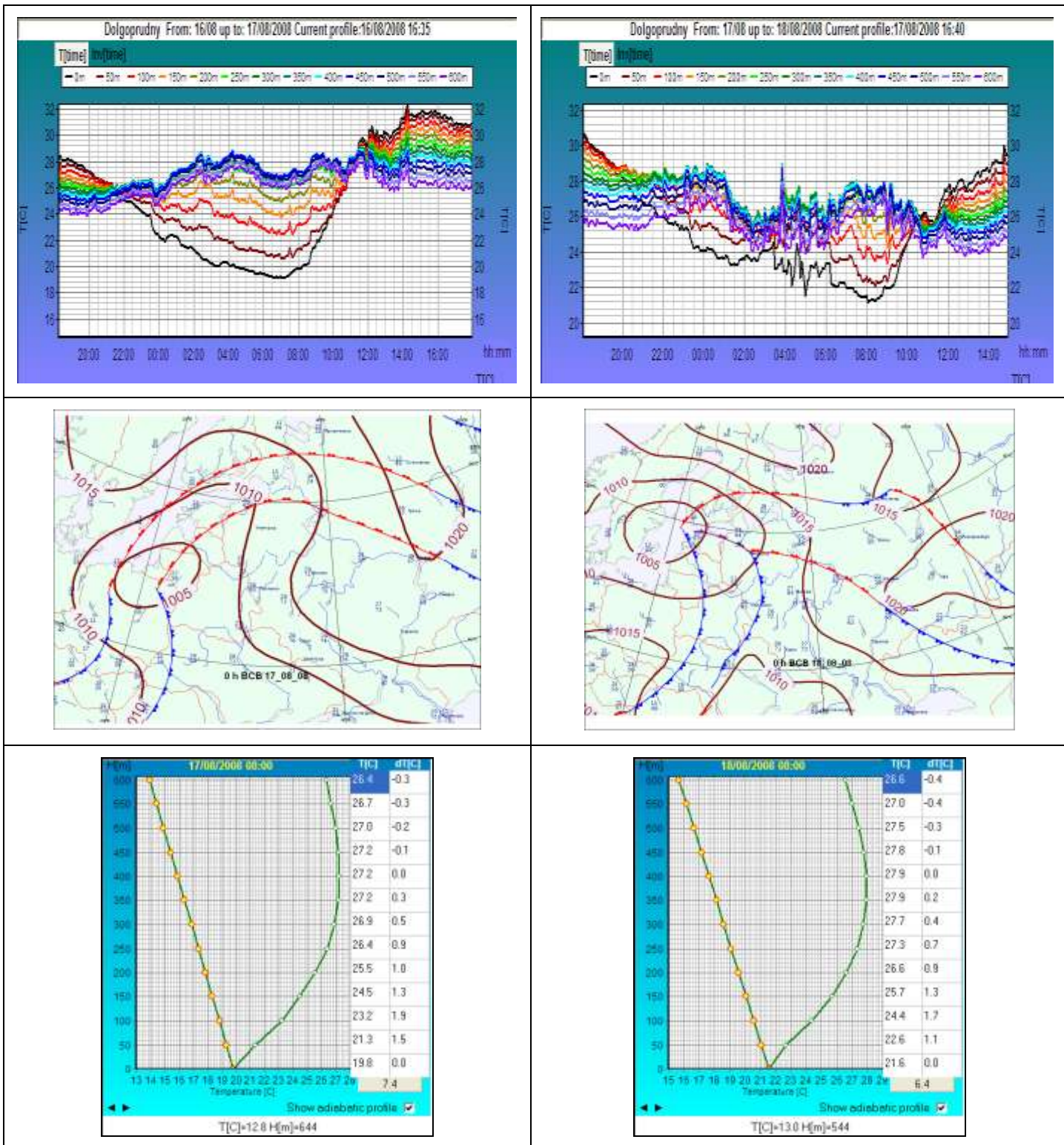


Fig. 26 Radiation temperature inversions: a typical surface inversion with a light wind in the lower atmosphere (on the left); surface inversion with internal structure disturbance by intensive turbulence (on the right). *In the second example, temperature oscillations in the inversion layer show that the influence*

of radiation inversion on pollution dissipation differs significantly from that of inversion with normal heat exchange processes.

The sharp temperature changes in a 400-600-m layer, in nighttime inversion, shown in Fig. 27, are an evidence of intensive vertical mixing (in this case, in the zone of a low-level jet stream).

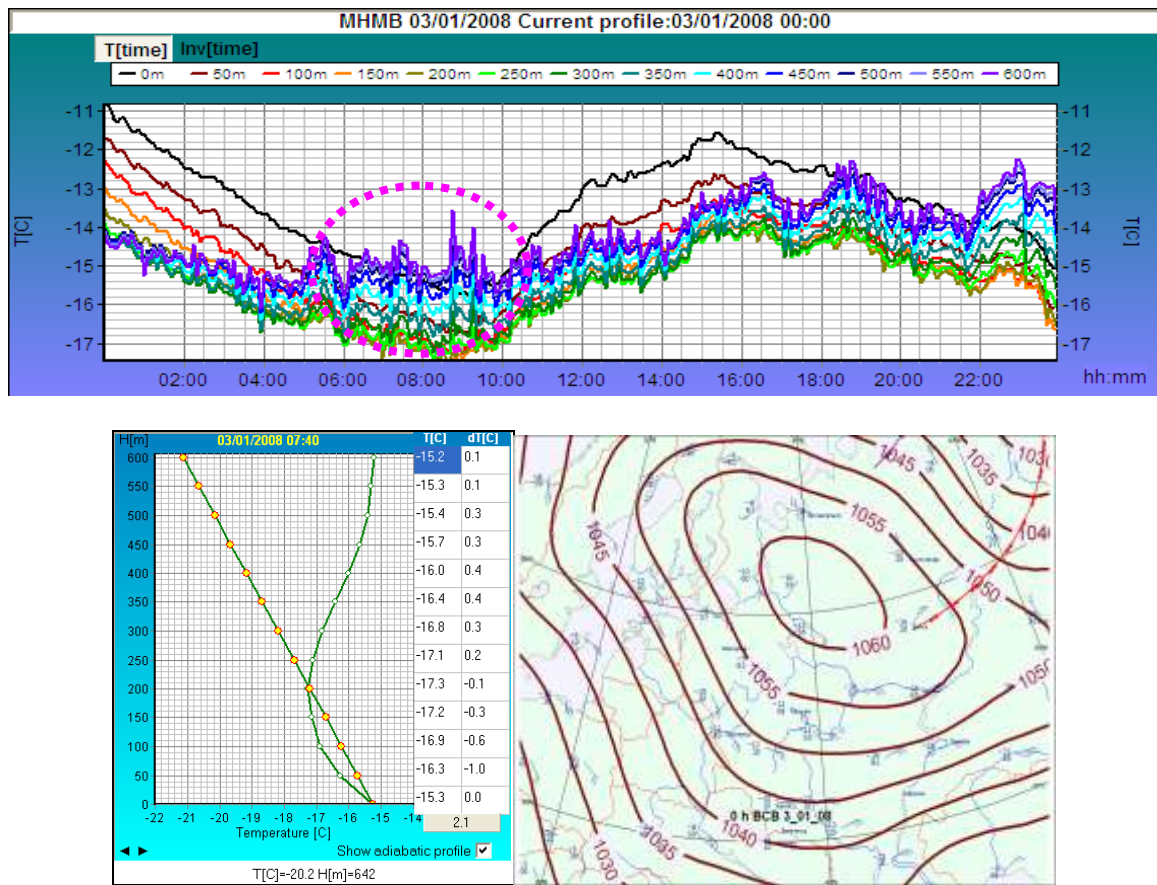


Fig. 27. Turbulence inversion (pink contour).

### c. Evaluate potential influence of internal urban air circulation on pollution dissipation

- At night, with light winds in the boundary atmospheric layer, conditions develop that favor the formation of an urban heat zone, the air circulation forced by it contributing to pollution transport and dissipation. It is recommended to use archived data to reveal the mechanism through which the urban heat zone affects the level of pollution in separate parts of the city, with its seasonal features and peculiarities specific to each particular city.

- To reveal the presence of a significant horizontal temperature gradient, using simultaneous radio sounding data from the nearest locality (the nearest suburb or city outskirts). It is also recommended to

compare vertical temperature gradients in the surface layer; large differences between them are indicative of differences in the urban thermal structure.

*In Moscow, e.g., with temperature differences in the surface layer and at a 300-m level over 3°C and 1°C, respectively, the transport in the lower atmosphere within the city zone considerably influences the concentration field formation, occasionally contributing to enhanced pollution in leeward city suburbs remote from pollution sources.*

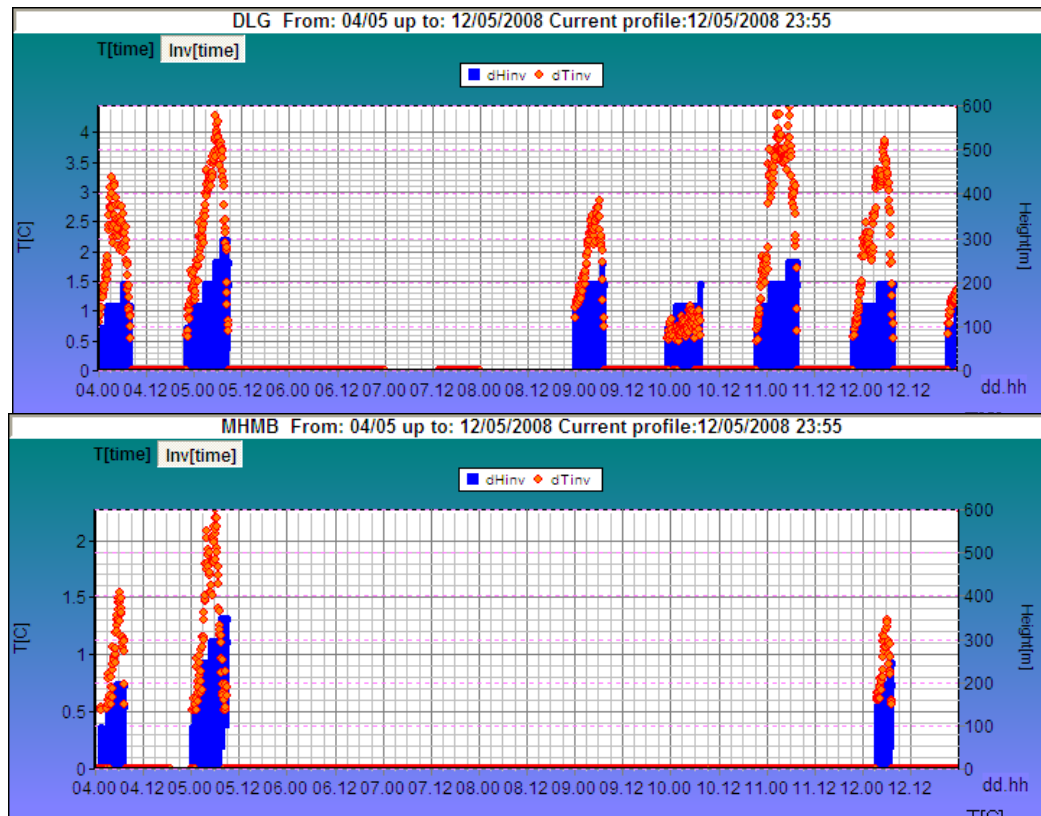


Fig. 28. Radiation temperature inversion features in the northern suburb (above) and the center of Moscow (below) on 4-12 May. Differences can be clearly seen between the inversion frequencies (the frequency in the city, during the period described, is twice as low), magnitudes (at maximum inversion development, the suburb magnitude is three times as high), and durations.

*According to Moscow observations, surface inversion frequency in the city center is on average three times less than in the nearest suburb and four times less than in the background area affected by Moscow heating.*

#### **d. Evaluate the potentials of temperature stratification persistence forecasting for the next night**

- Infer on the probability of the recurrence of similar thermal mixing conditions by summing up the data on thermal state characteristics of the night before, using prognostic information about the development of atmospheric processes;

- Establish the time of inversion formation and destruction (with corrections specific to a particular city allowed for), its magnitude and intensity, taking into account that thermal stability in surface atmospheric layers increases from night to night with stationary atmospheric processes.

**e. Allow for the specific features of diurnal thermal stratification variation**

The largest diurnal changes in surface air thermal stability are typical of warm periods: a transition from a nighttime thermal stability to morning instability occurs due to convection mixing development. In the afternoon, conditions leading to pollution removal from surface air are formed. The evening transition to steady stratification concurs with sunset, but the process in polluted atmosphere is delayed.

*In a warm season, in Moscow, e.g., the main minimum in the typical diurnal pollution change is observed in the afternoon, while the second one occurs between 01:00 and 05:00. The first pollution maximum is registered at 08:00 – 09:00, i.e., following meteorological conditions most unfavorable for pollution dissipation. This pollution maximum appears to be caused not only by morning peak motorway traffic emissions (the major air pollution source), but also by the preceding conditions that prevented pollution dissipation. An evening pollution maximum persists for a longer time period, generally, from 20:0 till 23:00. If, during the daytime, a mixing layer was not high and wind in the lower atmosphere was light, late at night, as thermal stability increases, pollution can be observed to increase due to the sinking of pollutants from the upper boundary layer portion.*

*In a cold season, the daytime layer of convection mixing is much less than the summer one; pollution dissipation conditions are mostly dependent on stratification and wind speed*

The features of pollution sources being specific to each particular city, it is recommended to define, using archived data, the relations between the type of thermal stability (in the preceding period) and pollution content in a representative zone of MTP-5 microwave measurements of temperature profiles. If a preliminary stage of comparison between radio sounding data (or mobile MTP-5 measurements) and simultaneous MTP-5 measurements shows a fairly good agreement, MTP-5 data can be conditionally assumed to characterize thermal structure for most of a city area.

## CONCLUSION

In 2002, the Hydrometeorological Center of the Russian Federation and the Central Aerological Observatory jointly developed “Instruction for the operational use of MTP-5 data for the monitoring of the boundary atmospheric layer state”, approved by the Central Commission for Instruments and Techniques of Roshydromet in 2004. The “Methodological Recommendations” presented is an updated version of the “Instruction...” extended to include analysis of the microwave measurements of temperature profiles; it does not give a description of the technical characteristics of the MTP-5 remote gage.

Temperature variation in the lower atmosphere is the result of large- and mesoscale processes. In big cities, a progressively more significant role in these processes belongs to anthropogenic forcing which causes changes in gas composition and radiation exchange, which, in turn, contribute to phenomena abnormal for the atmosphere of background regions (increase thermal instability, ‘urban’ inversions, circulation within urban heat zones, enhanced precipitation, etc

Information about the lower atmosphere processes lacking, the long-standing use of MTP-5 data in both operation activities and research has demonstrated the efficiency of the remote monitoring of the lower atmosphere thermal state as a means to study the boundary layer - the most variable part of the atmosphere.

In the first place, MTP-5 data enable detailed analysis of processes that occurred in the preceding time periods, deeper insight into phenomena that failed to be fully explored by conventional techniques. At the same time, they permit an early detection of the signs of changing weather and evaluate the probability of the formation of meteorological conditions favoring pollution accumulation both in a 24-hour forecast and diagnosis of conditions in the preceding period. The latter is no less important than the problem of forecasting as devising and further development of pollution forecasting methods should be based on highly reliable information about thermal stability, which is one of the main predictors of air pollution.

Due to the specific features of big cities, the relation between air pollution and thermal characteristics can vary. It is not impossible that some weather phenomena may show in the lower atmosphere temperature field, represented by MTP-5 data, in different ways.

The authors of the present ‘Recommendations...’ will appreciate any comments and requests of weather and pollution forecasters, as well as any references concerning phenomena observed in the MTP-5 visualized data for each measurement point, which are not described in this paper.

I.N. Kuznetsova:      [muza@mecom.ru](mailto:muza@mecom.ru)

E.N. Kadygrov:      [ldz@cao-rhms.ru](mailto:ldz@cao-rhms.ru)

E.A. Miller:          [tissary@rambler.ru](mailto:tissary@rambler.ru)

### Correspondence between stability grades and thermal stratification

Dynamic influence of an underlying surface on an air flow produces turbulence, which is increased or suppressed by stratification. Table 1 presents the characteristics of the correlation between the thermal state of the lower atmospheric layer and thermal stratification, obtained by researchers abroad (Pasquill and Turner) and by researchers from the Institute of Electric Engineering (IEE), under the guidance of N.L. Byzova.

Table 1. Quantitative correlation between stability grades and thermal stratification

Stratification characteristic	Stability evaluation method		
	By Pasquill	By Turner	Turner - IEE
Highly unstable	A	1	1
Moderately unstable	B	2	2
Slightly unstable	C	3	3
Neutral	D	4	4
Slightly stable	-	5	5
Moderately stable	E	6	6
Highly stable	-	7	7

Note that stability gradation was done with reference to turbulence intensity as applied to pollution dissipation calculations, i.e., unlike a small class of pollution dissipation conditions caused by convection mixing, a turbulent mixing mechanism is considered. The current stability classifications generally comprise 6-7 categories or classes (3 instability grades, 2-3 stability grades and a neutral one).

A deeper insight into pollution scattering processes should help explain some of the episodes of a low pollution level in the case of a low-height mixing layer of small magnitude evaluated conventionally either by comparison with the curve of the state or at stable stratification without inversion.

Table 2 gives the results of experimental observations from Obninsk weather tower and data processing results: a frequency distribution of the vertical temperature gradients in a 2-120-m layer, depending on stability grade, is presented

Table 2 – A frequency distribution of the vertical temperature gradients in a 2-120 m layer ( $T_2-T_{120}$ , Obninsk weather tower)

Stability grade	N	Temperature gradient, °C/100 m
-----------------	---	--------------------------------

<b>(by Turner-IEE)</b>		<b>3,5...2,6</b>	<b>2,5...1,6</b>	<b>1,5...0,6</b>	<b>0,5...-0,5</b>	<b>-0,6...-1,5</b>	<b>-1,6...-3,5</b>	<b>&lt;-3.5</b>
<b>Highly unstable</b>	<b>26</b>	<b>35</b>	<b>30</b>	<b>35</b>				
<b>Moderately unstable</b>	<b>66</b>	<b>33</b>	<b>48</b>	<b>15</b>	<b>1</b>		<b>3</b>	
<b>Slightly unstable</b>	<b>113</b>	<b>11</b>	<b>23</b>	<b>41</b>	<b>9</b>	<b>9</b>	<b>7</b>	
<b>Neutral</b>	<b>142</b>		<b>9</b>	<b>40</b>	<b>38</b>	<b>8</b>	<b>5</b>	
<b>Slightly stable</b>	<b>69</b>			<b>19</b>	<b>42</b>	<b>19</b>	<b>18</b>	<b>2</b>
<b>Moderately stable</b>	<b>76</b>			<b>4</b>	<b>18</b>	<b>18</b>	<b>42</b>	<b>18</b>
<b>Highly stable</b>	<b>106</b>			<b>1</b>	<b>5</b>	<b>7</b>	<b>28</b>	<b>59</b>

The data in Table 2 show a rather wide range of temperature gradients in the surface layer that refer to one and the same stability grade; this evidences the fact that processes of transport and scattering due to ordered motions and turbulence in the lower atmospheric layers do not fully explain all the mechanisms of heat exchange, and hence of pollution transport.

For practical purposes, in developing and evaluating schemes of weather and air pollution forecasts, it is recommended to use:

- an extended classification of stability grades, or
- quantitative predictors, namely, vertical gradient values in the lower 100-m atmospheric layer as most pollution sources are below a 100-m height.